*NMRF/VR/01/2023*

*VERIFICATION REPORT*

# NCUM Global Model Verification: October-November 2022

**K. Niranjan Kumar, M. Venkatarami Reddy, Sushant Kumar, Anumeha Dube, Mohana S. Thota, and Raghavendra Ashrit**

**2023**

**National Centre for Medium Range Weather Forecasting**
**Ministry of Earth Sciences, Government of India**
**A-50, Sector-62, NOIDA-201 309, INDIA**

# NCUM Global Model Verification: October-November 2022

**K. Niranjan Kumar, M. Venkatarami Reddy, Sushant Kumar, Anumeha Dube, Mohana S. Thota, and Raghavendra Ashrit**

***NMRF/VR/01/2023***

**National Centre for Medium Range Weather Forecasting**
**Ministry of Earth Sciences, Government of India**
**A-50, Sector 62, NOIDA-201309, INDIA**
**www.ncmrwf.gov.in**

**Data Control Sheet**

| | | |
|---|---|---|
| 1 | Name of the Institute | National Center for Medium range weather Forecasting, MoES, India |
| 2 | Document Number | NMRF/VR/01/2023 |
| 3 | Date of Publication | November 2023 |
| 4 | Title of the document | NCUM Global Monthly Verification: October-November 2022 |
| 5 | Type of the document | Verification Report |
| 6 | Number of pages, figures, and Tables | 37 pages, 29 figures, and 1 Table |
| 7 | Authors | K. Niranjan Kumar, M. Venkatarami Reddy, Sushant Kumar, Anumeha Dube, Mohana S. Thota, and Raghavendra Ashrit |
| 8 | Originating Unit | National Centre for Medium Range Weather Forecasting (NCMRWF), A-50, Sector-62, NOIDA201 309, India |
| 9 | Abstract | This report documents the analysis and forecasting performance of the global NCMRWF Unified Model (NCUM-G) during the Northeast monsoon season (ON) 2022. The verification results are presented to address (a) forecasters and (b) model developers. The information on biases in the forecasted winds, temperature, humidity, rainfall, etc., are crucial for the forecasters to interpret the model guidance for accurate forecasting. Furthermore, details on recent enhancements in the model's skill contribute to bolstering confidence in the accuracy of the model forecasts. |
| 10 | References | 15 |
| 11 | Security classification | Unrestricted |
| 12 | Distribution | General |

## Table of Contents

# NCUM Global Model Verification:

# October-November 2022

**K. Niranjan Kumar, M. Venkatarami Reddy, Sushant Kumar, Anumeha Dube, Mohana S. Thota, and Raghavendra Ashrit**

## सारांश

यह रिपोर्ट पूर्वोत्तर मानसून सीजन (अक्टूबर-नवंबर) 2022 के दौरान वैश्विक रा.म.अ.मौ.पू.कें. यूनिफाइड मॉडल (एन.सी.यू.एम.-जी) के विश्लेषण और पूर्वानुमान प्रदर्शन का दस्तावेजीकरण करती है। सत्यापन परिणाम (ए) पूर्वानुमानकर्ताओं और (बी) मॉडल डेवलपर्स को संबोधित करने के लिए प्रस्तुत किए जाते हैं। सटीक पूर्वानुमान के लिए मॉडल मार्गदर्शन की व्याख्या करने के लिए पूर्वानुमानित हवाओं, तापमान, आर्द्रता, वर्षा आदि में पूर्वाग्रहों की जानकारी पूर्वानुमानकर्ताओं के लिए महत्वपूर्ण है। इसके अलावा, मॉडल के कौशल में हालिया संवर्द्धन का विवरण मॉडल पूर्वानुमानों की सटीकता में विश्वास बढ़ाने में योगदान देता है।

## Abstract

This report documents the analysis and forecasting performance of the global NCMRWF Unified Model (NCUM-G) during the Northeast monsoon season (ON) 2022. The verification results are presented to address (a) forecasters and (b) model developers. The information on biases in the forecasted winds, temperature, humidity, rainfall, etc., are crucial for the forecasters to interpret the model guidance for accurate forecasting. Furthermore, details on recent enhancements in the model's skill contribute to bolstering confidence in the accuracy of the model forecasts.

# 1. Introduction

The performance of the global NCMRWF Unified Model (NCUM-G) forecasts during the October-November (ON) season of 2022 is presented in this report. The main aim of this assessment is to ascertain the accuracy and reliability of the forecasts through a comprehensive comparison with model analyses and observational data. The results are summarized for the post-monsoon season as a whole to understand the average biases and forecast performances. The report is oriented towards both (a) forecasters and (b) model developers. In section 2, the report outlines the NCUM-G model description and data assimilation system at NCMRWF along with detailing the observed data used in this report. Moving on to section 3,a thorough examination of the seasonal mean analysis and corresponding anomalies is presented, offering readers a comprehensive perspective on the model's performance throughout the northeast monsoon season. Section 4 of the report discusses the systematic biases observed in the forecasted large-scale upper fields such as wind, temperature, humidity, rainfall, etc., which are expected to be useful for the forecasters to interpret the model forecasts effectively. Section 5 subsequently provides a meticulous validation of the forecasts. Section 6 is devoted to the verification of significant weather events during the ON 2022 season. This encompasses the verification process for the Bay of Bengal cyclonic system (CS) ' SITRANG ' during 22-25 Oct 2022. Section 7 provides a concise summary of the obtained results.

# 2. NCMRWF Unified Modelling System & Verification datasets

## 2.1. Model Description

The NCMRWF started using the Unified Model (UM) Partnerships' seamless prediction system since 2012, naming this system as NCUM. The NCUM global Numerical Weather Prediction (NWP) system (NCUM-G) became operational in 2012 with a grid resolution of 25km (NCUM-G:V1) designed for medium-range weather prediction. This system underwent successive upgrades, progressing to a 17 km horizontal resolution (NCUM-G:V3) in 2015, followed by a refinement to a 12km resolution (NCUM-G:V5) in 2018. Further enhancements were made in 2020, resulting in a 12 km resolution coupled with improved model physics (NCUM-G:V6). The present version (NCUM-G:V7) of NCUM-G has a horizontal grid resolution of ~12 km with 70 levels in the vertical reaching 80 km height. It uses "ENDGame" dynamical core, which provides improved accuracy of the solution of primitive model equations and reduced damping. This helps in producing finer details in the simulations of synoptic features such as cyclones, fronts, troughs, and jet stream winds. ENDGame also increases variability in the tropics, which leads to an improved representation of tropical cyclones and other tropical phenomena. The model uses improved physics options of GA7.2 (Walters et al., 2017). An advanced data assimilation method of Hybrid 4-Dimensional Variational (4D-Var) is used

for the creation of NCUM global analysis. The advantage of the Hybrid 4D-Var is that it uses a blended background error, a blend of "climatological" background error, and day-to-day varying flow dependent background error (derived from the 22–member ensemble forecasts). The hybrid approach is scientifically attractive because it elegantly combines the benefits of ensemble data assimilation (flow-dependent co-variances) with the known benefits of 4D-Var within a single data assimilation system (Barker, 2011). A brief description of the NCUM Hybrid 4D-Var system is given in Kumar et al. (2021, 2020, & 2019).

### 2.2. Observed/analysis Data used for the Verification

The seasonal mean analysis and anomalies are studied using the fifth-generation European Centre for Medium-Range Weather Forecasts (ECMWF) reanalysis product (ERA-5) (Hershbach et al. 2020) climatology (1979-2018). The high resolution (12km) NCUM-G analysis data is interpolated to ERA-5 grid resolution ($0.25^0$x$0.25^0$). For verification of the forecasts, the NCUM-G model analysis is used. All systematic errors are computed at a native grid resolution of 12km.

Detailed quantitative rainfall forecast verification is based on the India Meteorological Department (IMD)-NCMRWF daily high resolution ($0.25^0$) rainfall analysis (Mitra et al. 2009, 2013). The rainfall analysis objectively analyses India Meteorological Department (IMD) daily rain gauge observations onto a $0.25^0$ grid using a successive corrections technique with the GPM Satellite rainfall providing the first guess estimates. The model forecasts are gridded to the $0.25^0$ observed rainfall grids over Indian land regions for 61 days from 1st October 2022 to 30st November 2022. As noted by Mitra et al. (2009), the merged analysis at $0.25^0$ grid resolution is appropriate for capturing the large-scale rain features associated with the monsoon. The merging of the IMD gauge data into GPM estimates not only corrects the mean biases in the satellite estimates but also improves the large-scale spatial patterns in the satellite field, which is affected by temporal sampling errors (Mitra et al. 2009). Verification of daily temperature forecasts is carried out against the IMDs daily observed gridded ($0.5^0$ x $0.5^0$) maximum (Tmax) and minimum (Tmin) temperature data (Srivastava et al. 2009).

## 3. NCUM-G Analysis Mean and Anomalies during ON 2022

### 3.1. Winds at 850, 700, 500, and 200 hPa levels

The NCUM-G mean analysis fields and anomalies relative to climatology are assessed in this section during Oct-Nov 2022. The discussion is presented for Winds, Temperature, and Relative Humidity at four standard pressure levels of 850, 700, 500, and 200 hPa. The anomalies are computed against the ERA5 climatology (1979-2018).

During Oct-Nov 2022 season, the reversal of winds across India in contrast to summer seasons (June through September, JJAS), and a significant amount of rainfall in the southeastern part of peninsular India are the major features (Rajeevan et al. 2012). Here, we first discuss the mean winds and anomalies at 850 and 700 hPa levels from NCUM-G analysis that are shown in Figures 1a-d. The 850 hPa wind pattern suggests the prevailing easterly/northeasterly winds towards south peninsular India during Oct-Nov 2022 season (Figure 1a). This seasonal reversal of winds is partly associated with the development of high-pressure cells over the Tibetan and Siberia Plateaus, and the southward movement of the Inter Tropical Convergence Zone (ITCZ). It also noted that the strong westerly flow is prominent over the equatorial Indian Ocean. Another important feature is the establishment of a trough in the southern Bay of Bengal (BoB) and associated with that we could see a cyclonic circulation. This trough draws tropical disturbances such as cyclones and easterly waves causing the perturbation in the wind field subsequently progressing westward resulting in widespread rainfall over south India. At 700 hPa (Figure 1b) similar features are noted in the mean winds relative to 850 hPa winds. The anomalous winds during the Oct-Nov 2022 season relative to ERA5 climatology are shown in Figures 1c and 1d. The anomalous winds at 850 and 700 hPa show enhanced westerly flow over the equatorial Indian Ocean. Over the Indian land region, anomalous southerlies (weakened northerly mean winds) are prominent at 700 hPa. In addition, the anomalous winds suggest an anomalous cyclonic circulation over south BoB. Similar features in the anomalous flow for ON 2022 can be noticed at 700 hPa level.

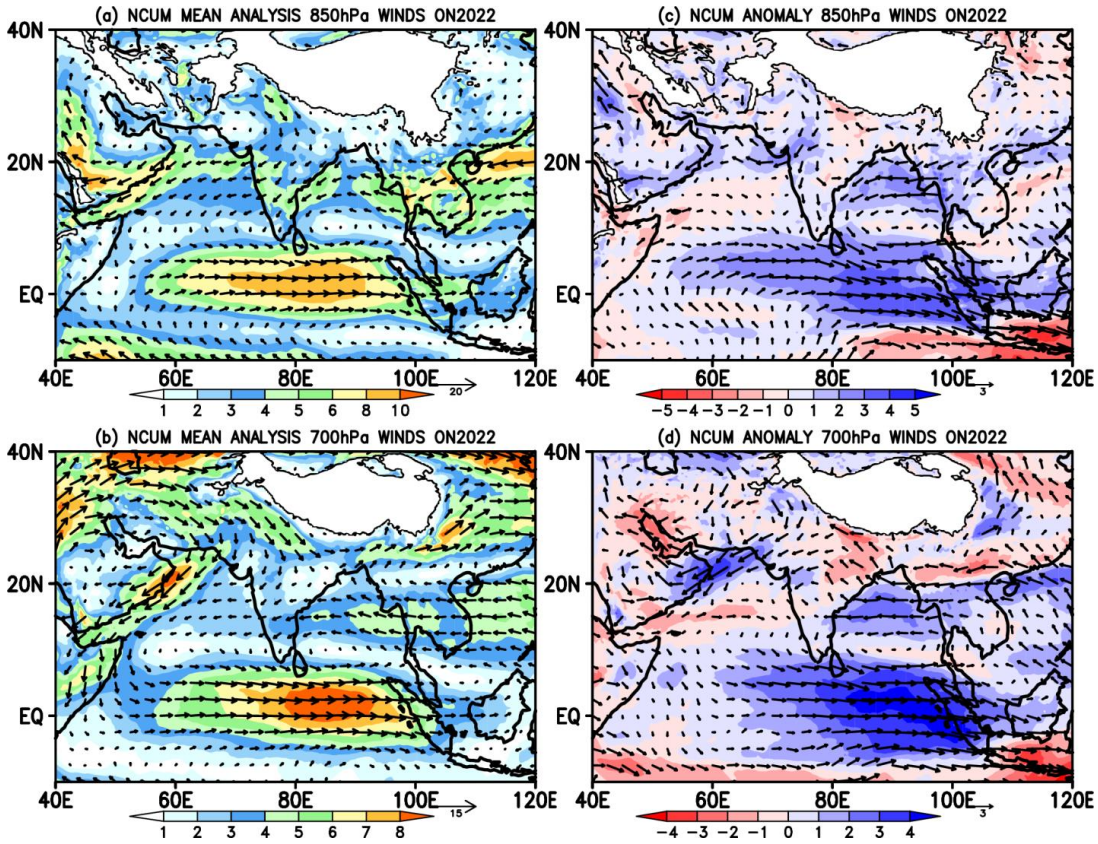


**Figure 1. Mean winds at (a) 850 hPa and (b) 700 hPa in the NCUM-G Analysis during ON 2022 (m/s). Right panels show the anomaly circulations at (c) 850 hPa and (d) 700 hPa.**

The mid- and upper- tropospheric mean winds and corresponding anomalies from ERA5 climatology are shown in Figure 2. One of the main synoptic features is the subtropical westerlies between 20-40$^0$N. At 500 hPa, the deflection of westerlies between 20-40$^0$N and 80-100$^0$E can be seen in the mean winds due to Himalayan topography. The strength of these westerlies is increased from 500 hPa to 200 hPa. The subtropical jet (STJ) is clearly visible/seen at 200 hPa (Figure 2b) with magnitudes more than 40m/s. At the same time over the southern region reduction in the strength of easterlies can be seen at 200 hPa level. Further, the associated anomalous wind flow for the ON 2022 in the mid- and upper troposphere is presented in Figures 2c and 2d. The enhanced easterly over south India is clearly observable, while, simultaneously, the magnitudes of winds in central and north India are lower than the climatology at 500hPa (Figure 2c). At 200hPa level contrasting features are noted in the intensity of the STJ (Figure 2d). The tropical easterlies on the other hand indicate above normal with magnitudes of about 5-6m/s.

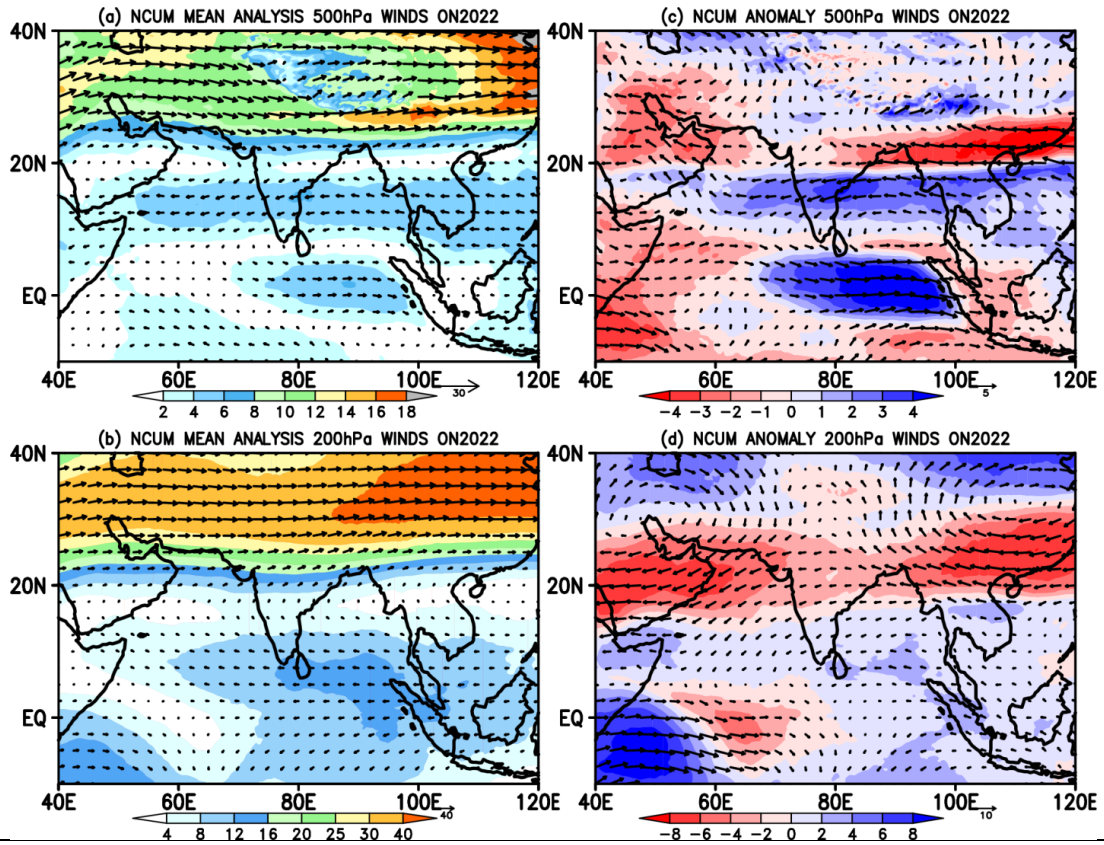


**Figure 2. Mean winds at (a) 500 hPa and (b) 200 hPa in the NCUM-G Analysis during ON 2022 (m/s). Right panels show the anomaly circulations at (c) 500 hPa and (d) 200 hPa.**

## 3.2. Temperature at 850, 700, 500, and 200 hPa levels

The spatial distribution of seasonal mean temperatures in the lower troposphere is shown in Figures 3a and 3b. The mean daily temperature at lower levels (i.e., at 850 hPa) exceeds $18^0$C over the western Indian regions (Figure 3a). In contrast to the temperatures at 850 hPa level, the temperature distribution is quite homogeneous ranging between 8-$10^0$C, except over the BoB at 700 hPa. This relatively strong heating in the lower troposphere probably enhances the trough and subsequently, the cyclogenesis noted earlier. The anomalous temperature distribution is indicated in Figures 3c and 3d. The temperature anomalies reveal that the above-normal temperature over BoB relative to climatological means with magnitudes of $1^0$C is favorable for convective initiation over BoB.

The spatial distribution of mid- and upper-tropospheric temperatures and corresponding anomalies with respect to the seasonal mean climatology is shown in Figure 4. The seasonal mean temperature at 500 hPa during ON 2022 indicates quite uniform over the Indian subcontinent and adjoining seas (Figure 4a). However, it clearly noticed that the upper tropospheric temperature, specifically over the Tibetan Plateau is

quite high (Figure 4b). On the other hand, the anomalous features (Figures 4c and 4d) indicate the above-normal temperatures over almost entire domain at 500 and 200 hPa.

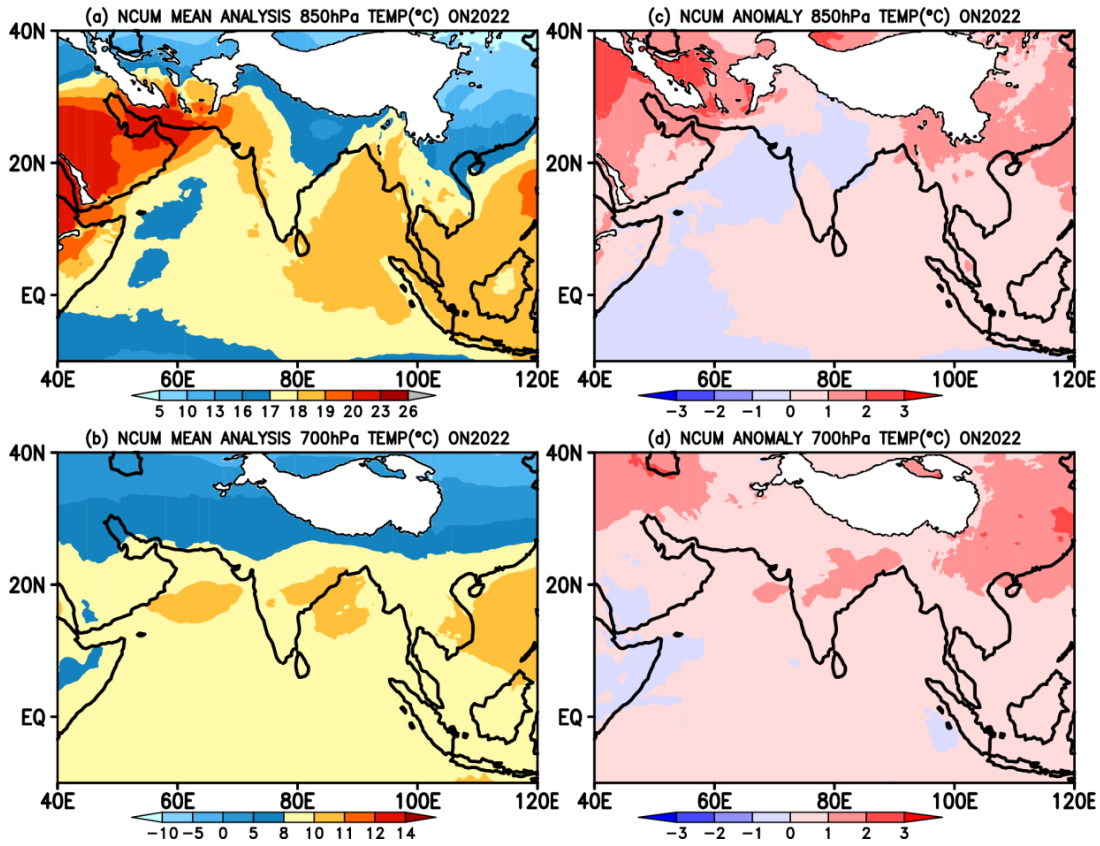


**Figure 3. Mean Temperature (Degree Celsius, $^{0}$C) at (a) 850 hPa and (b) 700 hPa in the NCUM-G Analysis during ON 2022. Right panels show the Temperature anomalies at (c) 850 hPa and (d) 700 hPa.**

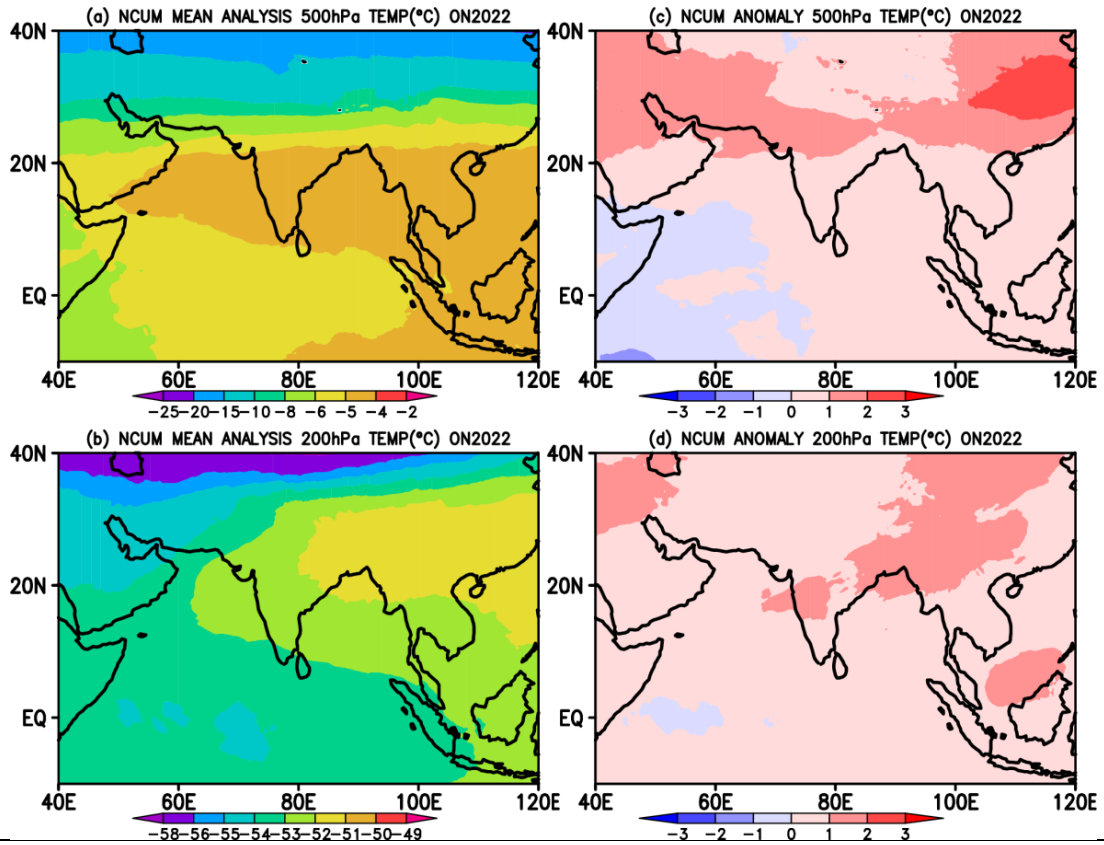


**Figure 4. Mean Temperature (Degree Celsius, $^0$C) at (a) 500 hPa and (b) 200 hPa in the NCUM-G Analysis during ON 2022. Right panels show the Temperature anomalies at (c) 500 hPa and (d) 200 hPa.**

### 3.3. Relative Humidity (RH) at 850,700, and 500 hPa levels

The spatial distribution of humidity is an important field along with wind and temperature for its influence on the rainfall. In Figure 5, we showed the spatial distribution of seasonal mean humidity and consequent anomalies in the lower troposphere. It is clearly noticed from Figure 5a that the lower tropospheric humidity is larger over the southern peninsula India. This could be associated with the strong easterly flow from BoB to the Indian subcontinent during North-East Monsoon (NEM) and rainfall spells associated with the easterly waves. There is a significant amount of difference between the north and south of India w.r.t the magnitudes of RH at both 850 hPa and 700 hPa levels. Also, the high humidity can be noticed over the equatorial Indian Ocean and Maritime Continent (MC). In particular, when we see the anomalous distribution for the ON 2022, the below-normal percentage of RH can be clearly visible over the entire Indian land region and neighbouring seas excluding Arabian Sea (AS) and head BoB at 850 hPa. As we move to the 700 hPa level, we can see the decrease in RH over southern peninsular India (Figure 5b), nevertheless, the anomalies indicate the below-normal values across the entire Indian land region and above-normal over the surrounding oceanic regions excluding northern AS for the ON 2022. A similar spatial structure in RH at 500 hPa level is also noted in NCUM-G. Further, the RH anomalies indicate above-normal over BoB and coastal regions around the south

peninsular India (Figure 6b). Hence, this above-normal RH (see Figures 5 and 6) during ON 2022 in the lower troposphere to mid-troposphere contributes to excess rainfall amounts over BoB and southern peninsular India in NCUM-G, which will be seen in Section 5.

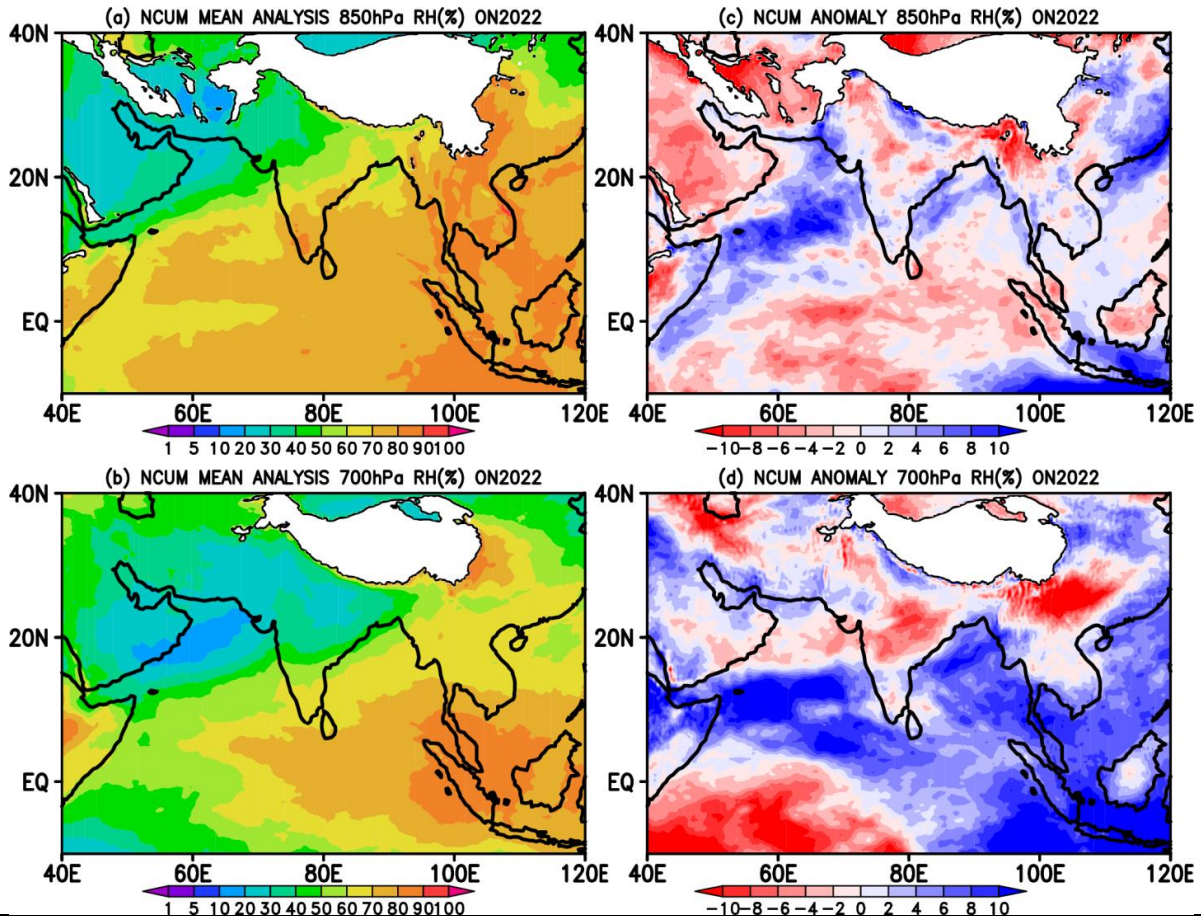


**Figure 5. Mean Relative Humidity (%) at (a) 850 hPa and (b) 700 hPa in the NCUM-G Analysis during ON 2022. The right panels show the anomalies in Relative Humidity at (c) 850 hPa and (d) 700 hPa.**

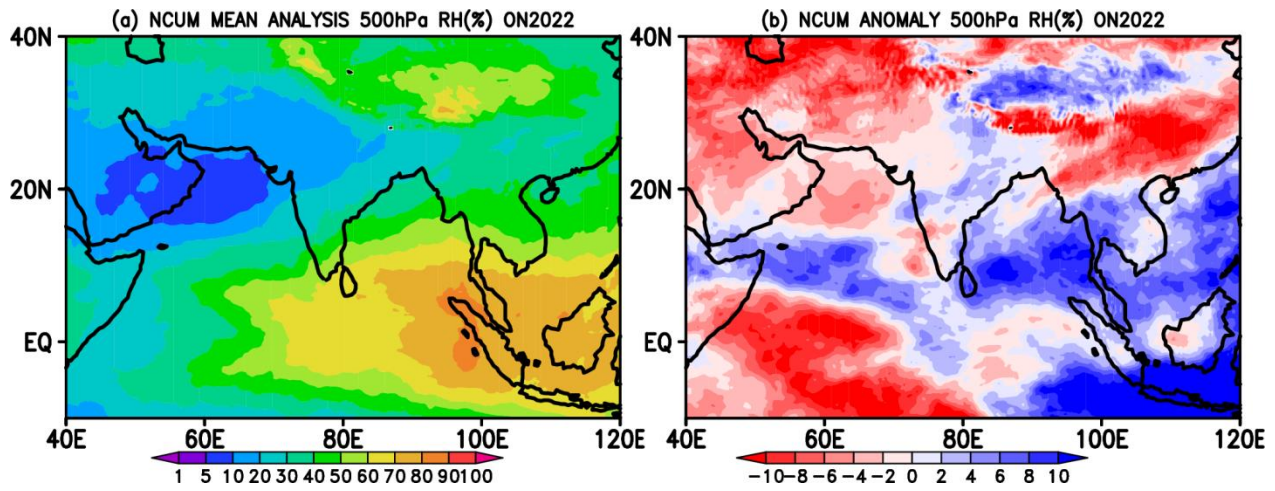


**Figure 6. Mean Relative Humidity (%) (a) Mean and (b) anomaly at 500 hPa in the NCUM-G Analysis during ON 2022.**

## 4. Systematic Errors in NCUM-G Forecasts

In this section a brief description about systematic errors in Day-1 (24 hr), Day-3 (72 hr), and Day-5 (120 hr), forecasts during October and November (ON) 2022 are given. The forecast errors with respect to model analysis are presented for Winds, Temperature, and Relative Humidity at 850, 700, 500, and 200 hPa levels (Figures 7-18).

### 4.1. Winds at 850,700, 500, and 200 hPa levels

Mean winds at 850 hPa level show the presence of low-level north-easterlies over central India and parts of Arabian Sea. A feeble cyclonic circulation is seen over Bay of Bengal with easterlies and westerlies on north and southern planks, respectively. The presence of north-easterly winds along the eastern part, especially over Southeast India indicates the effect of NEM during this season. Maximum northeasterly winds are seen along the coastal regions of Somali and South China Seas region. In addition, the presence of strong westerly winds along the equator is also noted (Figure 7a). Systematic errors in winds from Day-1 forecasts at this level show an easterly wind bias along equator around 80-100$^0$E. A westerly wind bias over the south Arabian Sea around 60$^0$E is seen in Day-1 forecast which is getting enhanced with forecast lead time. Errors in low-level winds enhance around the equatorial regions and this could be due to the enhanced convective activity during the winter season (Figures 7 c-d). Similar systematic errors in winds are also noticed at 700 hPa level. Interestingly Day-1 forecast errors are relatively small compared to the Day-3 and Day-5 forecasts. In addition, westerly wind bias is more prominent at 700 hPa level over central India in Day-3 and Day-5 forecasts (Figures 8 c-d).

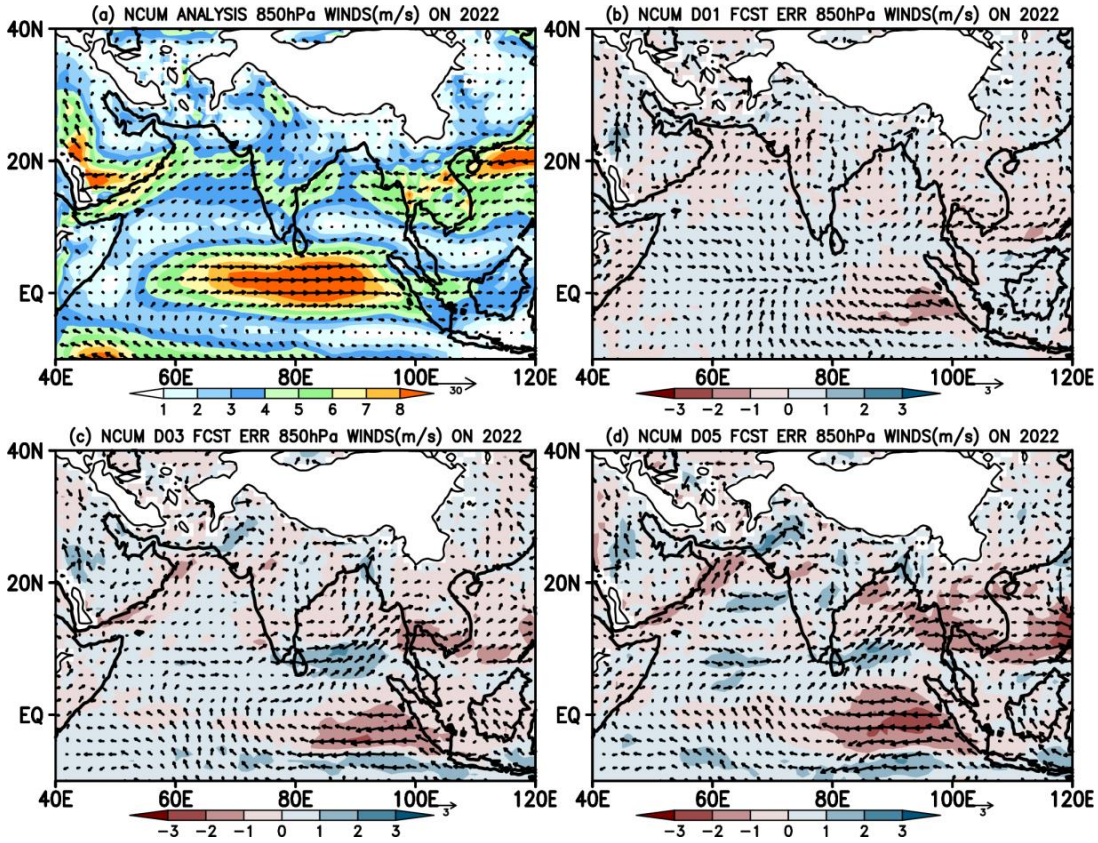


**Figure 7. (a) Mean winds and systematic errors (m/s) in (b) Day-1, (c) Day-3, and (d) Day-5 forecasts at 850 hPa during ON 2022.**

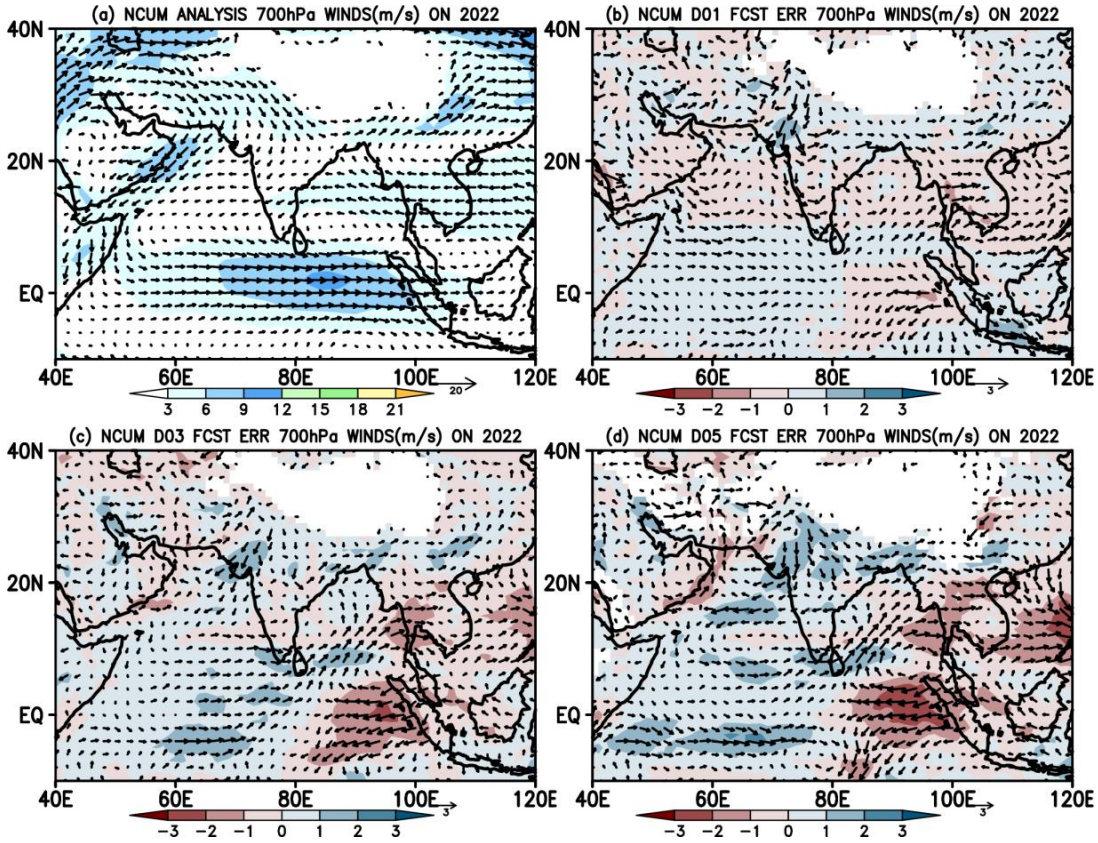


**Figure 8. (a) Mean winds and systematic errors (m/s) in (b) Day-1, (c) Day-3, and (d) Day-5 forecasts at 700 hPa during ON 2022.**

Mean winds at 500 hPa level show strong westerlies between 30-40$^0$N and these winds penetrated over the central Indian region and turning of winds to north easterlies over AS. In addition, the presence of strong easterlies over BoB is also noted (Figure 9a). Errors in winds at 500 hPa level are relatively small in Day-1 forecasts. The wind bias seen over equatorial regions is enhancing in Day-3 and Day-5 forecasts with westerlies on the west and easterlies on the eastern indicating active convection around equatorial regions. The enhanced winds exhibit cyclonic circulation over south AS just above the equator in Day-3 and Day-5 forecast around 500 hPa level, which is noteworthy (Figures 9 c-d). Systematic errors at 200 hPa level winds show enhanced divergent circulation along the equatorial regions on Day-3 and a similar spatial pattern in winds is also seen on Day-5 with enhanced error magnitudes (Figures 10 c-d)

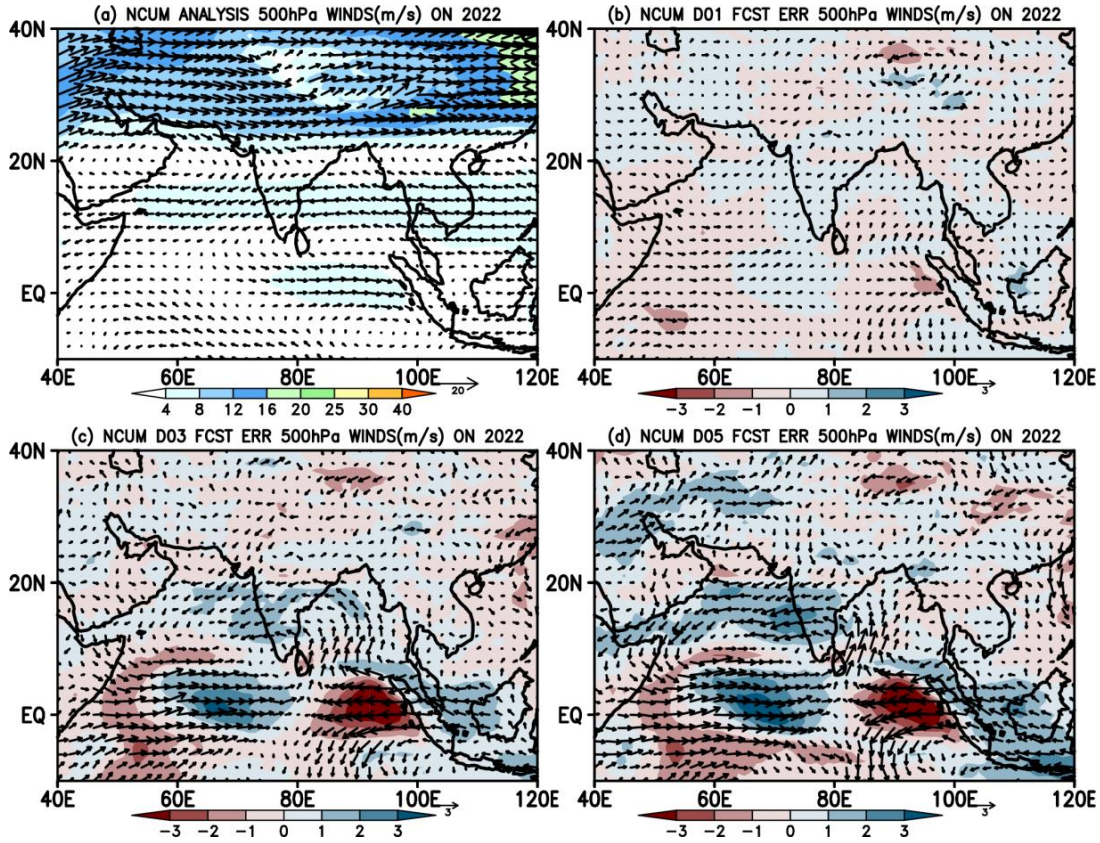


**Figure 9. (a) Mean winds and systematic errors (m/s) in (b) Day-1, (c) Day-3, and (d) Day-5 forecasts at 500 hPa during ON 2022.**

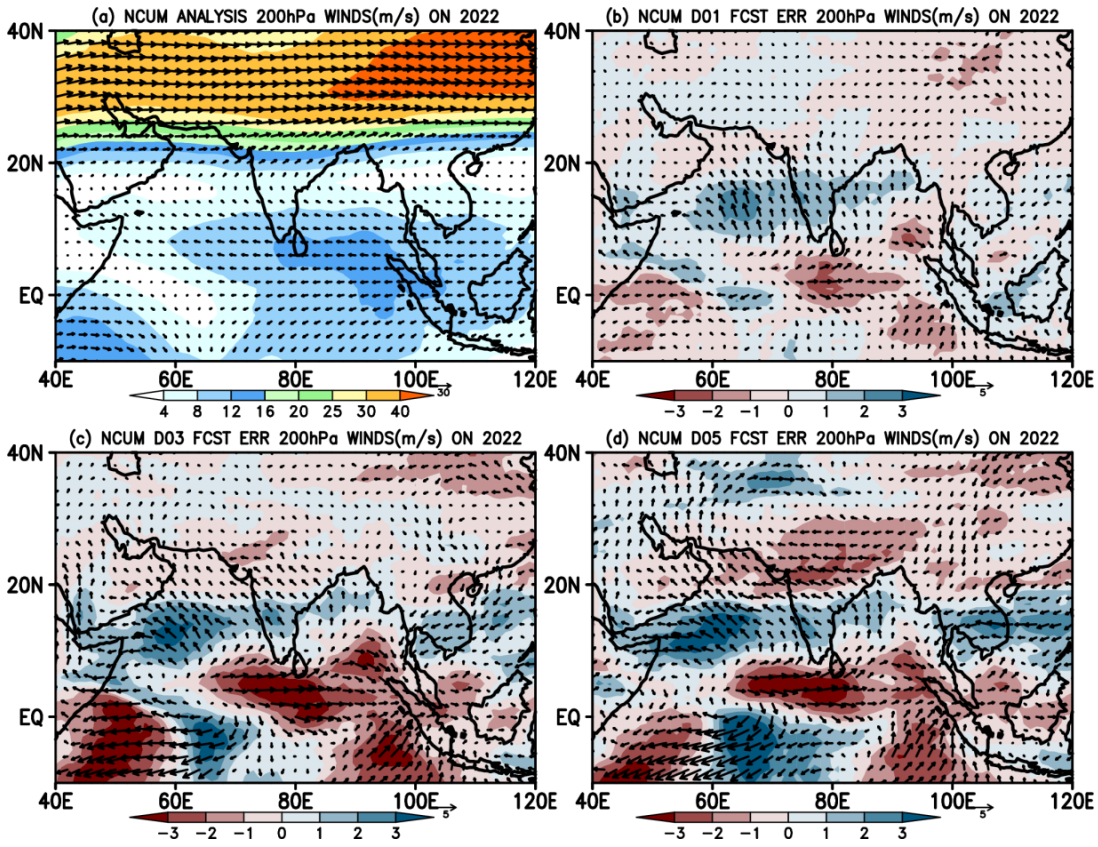


**Figure 10. (a) Mean winds and systematic errors (m/s) in (b) Day-1, (c) Day-3, and (d) Day-5 forecasts at 200 hPa during ON 2022.**

## 4.2. Temperature and Relative Humidity

Spatial map of seasonal mean temperature from NCUM-G analysis at 850 hPa shows relatively warm temperatures (18-20$^0$C) over BoB, parts of AS, and surrounding oceanic regions (Figure 11a). The Model shows warm bias (~1$^0$C) occupied over northwestern Indian land mass and also over the oceanic regions, and the magnitude of this bias is increasing over land regions with forecasts lead time (Figure 11 b-d). These error increments at 850 hPa temperatures are also more prominent over eastern African regions. On a similar note, the temperature at 700 hPa (Figures 12 b-d) also shows warm bias (~0.5$^0$C) over most of the Indian land region except a small portion over South peninsular India. Interesting to see that the bias over equatorial oceanic regions reverse sign and now exhibits cold bias compared to the 850hPa level. This cold bias over oceanic regions exhibits a slight increment with forecast lead time (Figures 12 b-d). At 500 hPa level, temperature exhibits warm bias over most of the Indian land mass including surrounding oceanic regions, and the magnitude of the bias is increasing in forecasts with lead time (Figures 13 b-d). However, errors in upper-troposphere (200 hPa) temperatures (Figures 14-b-d) over the Indian land region and most of the Indian Ocean show cold bias. A large patch of warm bias (~0.5$^0$C) over the eastern equatorial Indian Ocean (EEIO) is prominent and is moving slightly eastward in Day-3 and Day-5 forecasts.

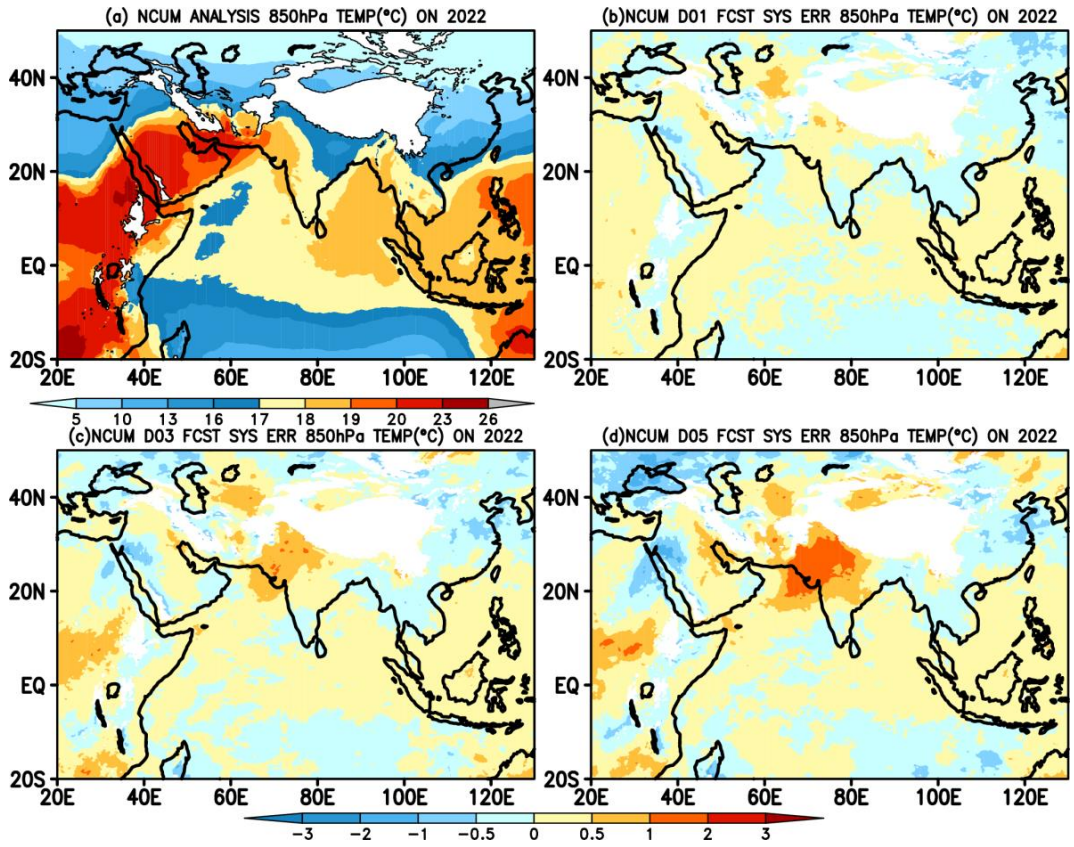


**Figure 11. (a) Mean Temperature (Degree Celsius, $^0$C) and systematic errors (Degree Celsius, $^0$C) in (b) Day-1, (c) Day-3, and (d) Day-5 forecasts at 850 hPa during ON 2022.**

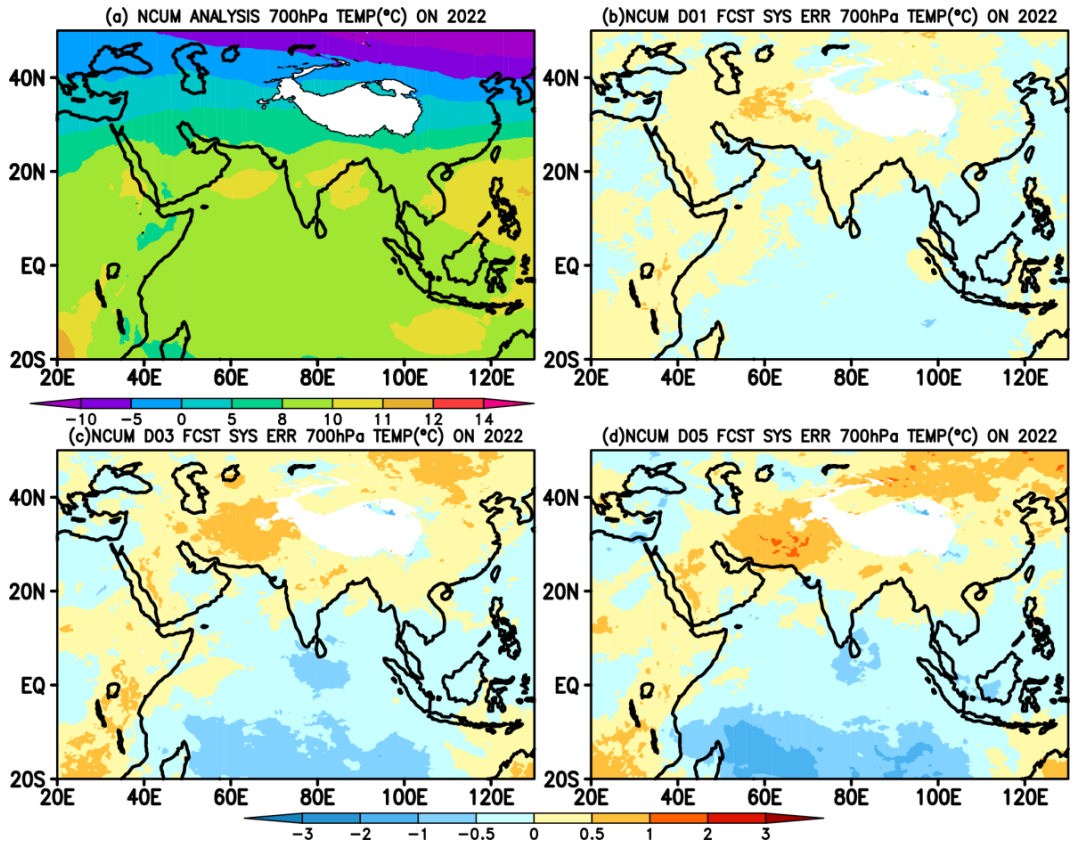


**Figure 12. (a) Mean Temperature (Degree Celsius, $^0$C) and systematic errors (Degree Celsius, $^0$C) in (b) Day-1, (c) Day-3, and (d) Day-5, forecasts at 700 hPa during ON 2022**

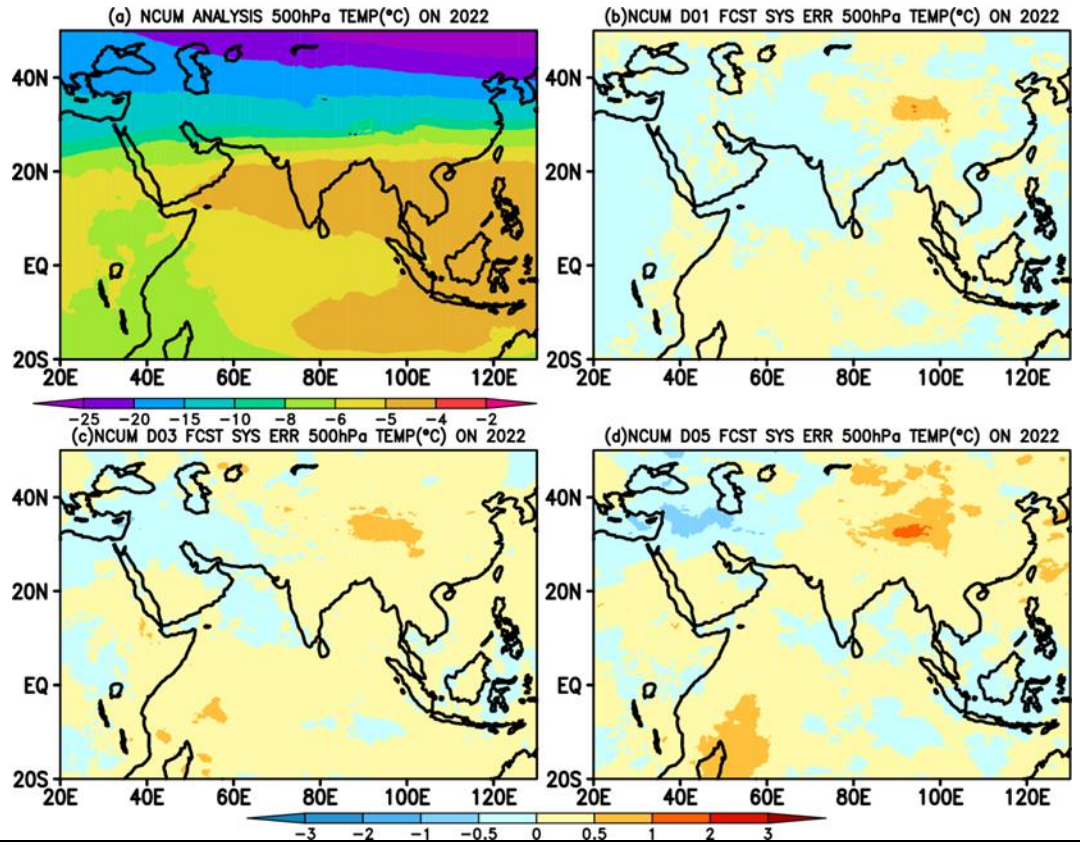


**Figure 13. (a) Mean Temperature (Degree Celsius, $^0$C) and systematic errors (Degree Celsius, $^0$C) in (b) Day-1, (c) Day-3, and (d) Day-5 forecasts at 500 hPa during ON 2022.**

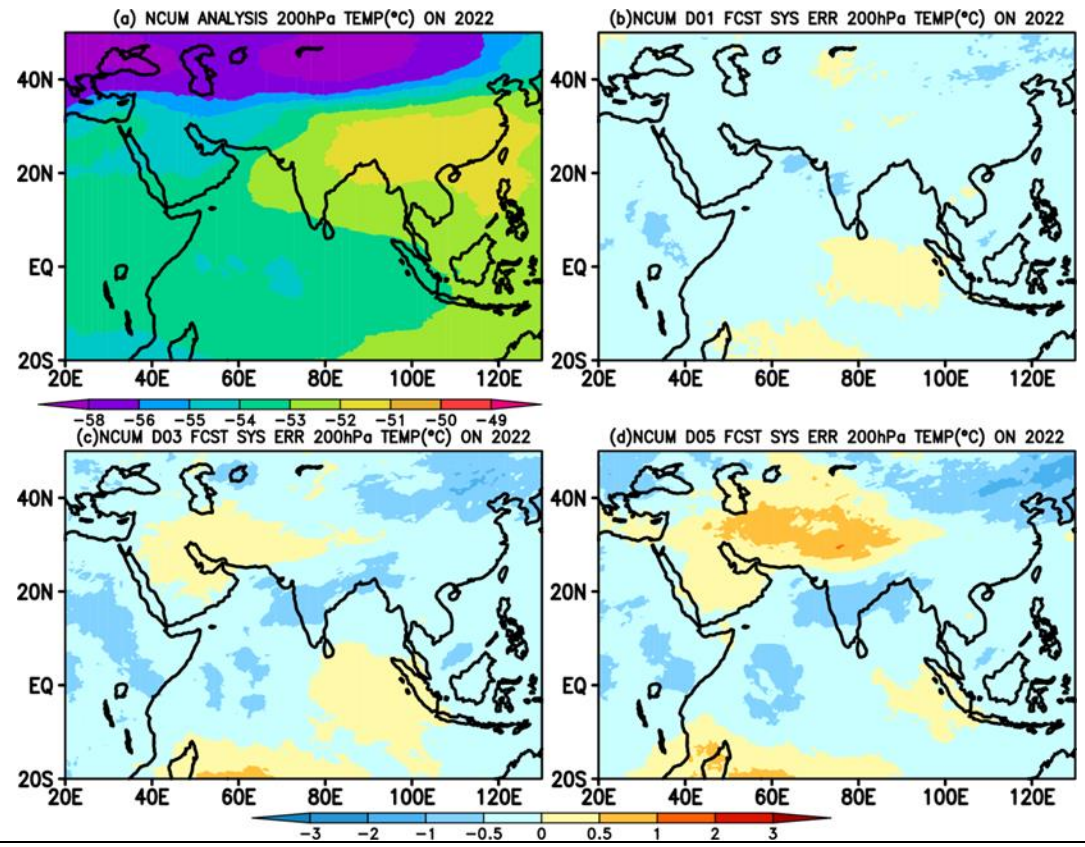


**Figure 14. (a) Mean Temperature (Degree Celsius, $^0$C) and systematic errors (Degree Celsius, $^0$C) in (b) Day-1, (c) Day-3, and (d) Day-5 forecasts at 200 hPa during ON 2022.**

Seasonal mean RH at 850 (Figure 15a) and 700 hPa (Figure 16a) levels show large values > 90% over eastern parts of the Indian subcontinent and over the Maritime Continent (MC) regions, and relatively lower RH (dry) values over the northwestern parts of India. Maximum RH values are concentrated over MC consistent with the active convection during the winter period. Systematic errors at 850 hPa level show dry bias over the Indian land region, most of the Indian subcontinent, and regions surrounding MC; and this dryness is enhancing with forecasts lead time (Figures 15 c-d), which could possibly influence the MJO propagation through MC in NCUM-G. Interestingly the dry bias observed over the Indian land region at 850 hPa level changed sign to positive and moist bias is seen at 700 hPa level (Figures 16 b-d). However, the dryness over MC and surrounding regions still persists at all the levels from 700 to 200 hPa (Figures 16, 17, and 18). In contrast, the moist bias south of the equator is getting intensified in the Day-3 and Day-5 forecast, and the entire column is occupied with excess moisture from 700 to 500 hPa levels (Figures 16 and 17). At 200 hPa, RH exhibits dry bias over the northwestern Indian region, northern AS, and the south of the equator. Notably, these dry biases become more pronounced with an increase in forecast lead time, as illustrated in Figures 18 c-d.

In the next section, a brief description of systematic errors in the model forecasts is presented for key surface variables such as 2m Temperature (Figure 19), 10m winds (Figure 20), and Total Precipitable water (PWAT; Figure 21). The errors are computed against the NCUM-G analysis.

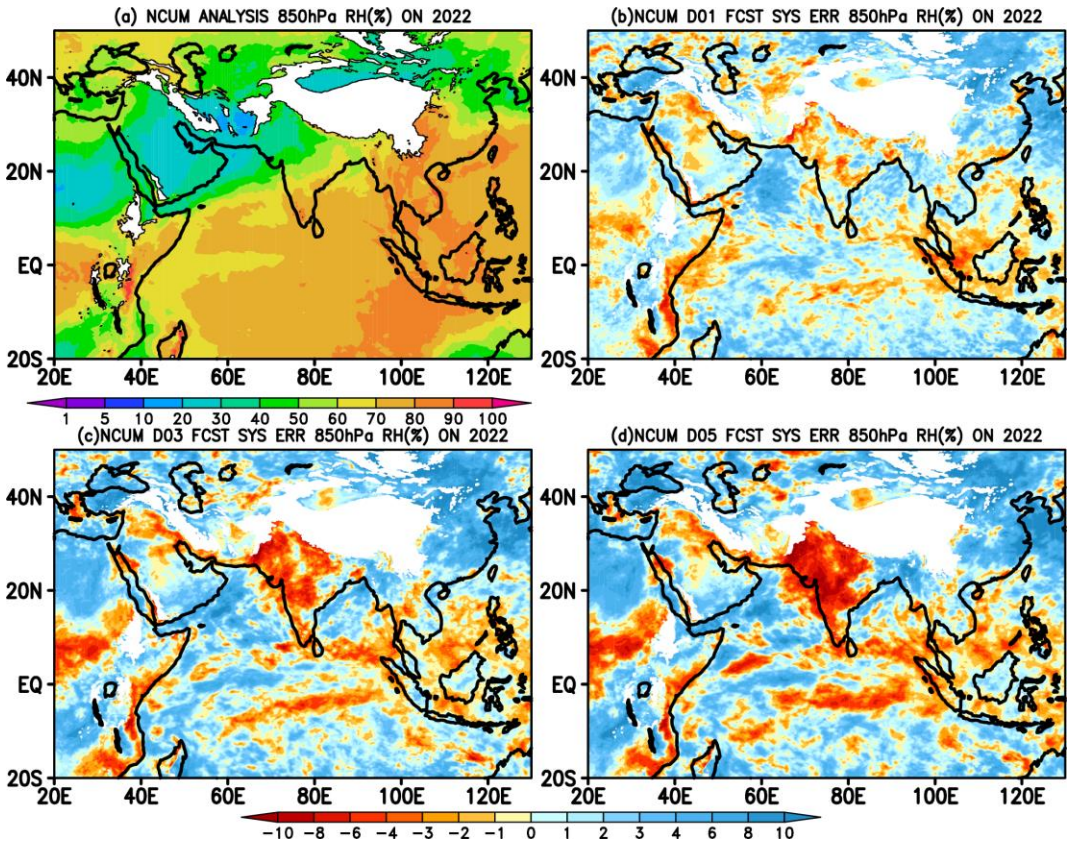


**Figure 15. (a) Mean Relative Humidity (%) and systematic errors (%) in (b) Day-1, (c) Day-3, and (d) Day-5 forecasts at 850 hPa during ON 2022.**

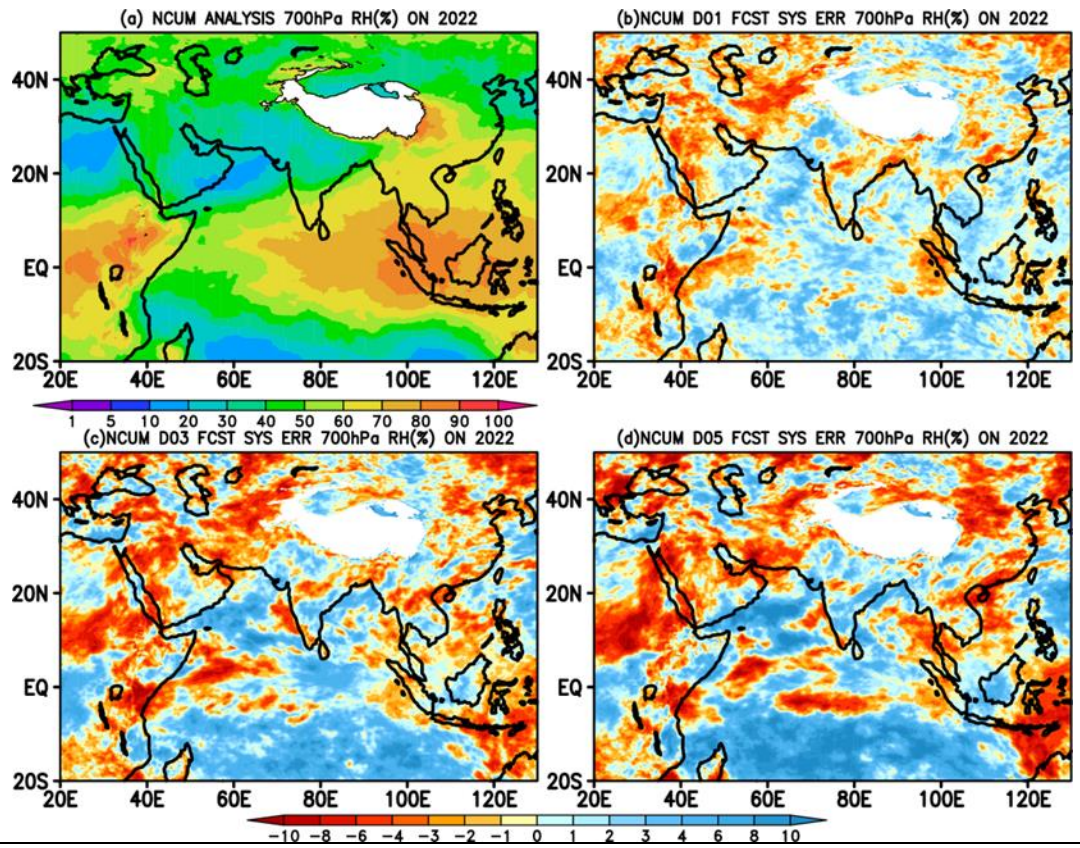


**Figure 16. (a) Mean Relative Humidity (%) and systematic errors (%) in (b) Day-1, (c) Day-3, and (d) Day-5 forecasts at 700 hPa during ON 2022.**

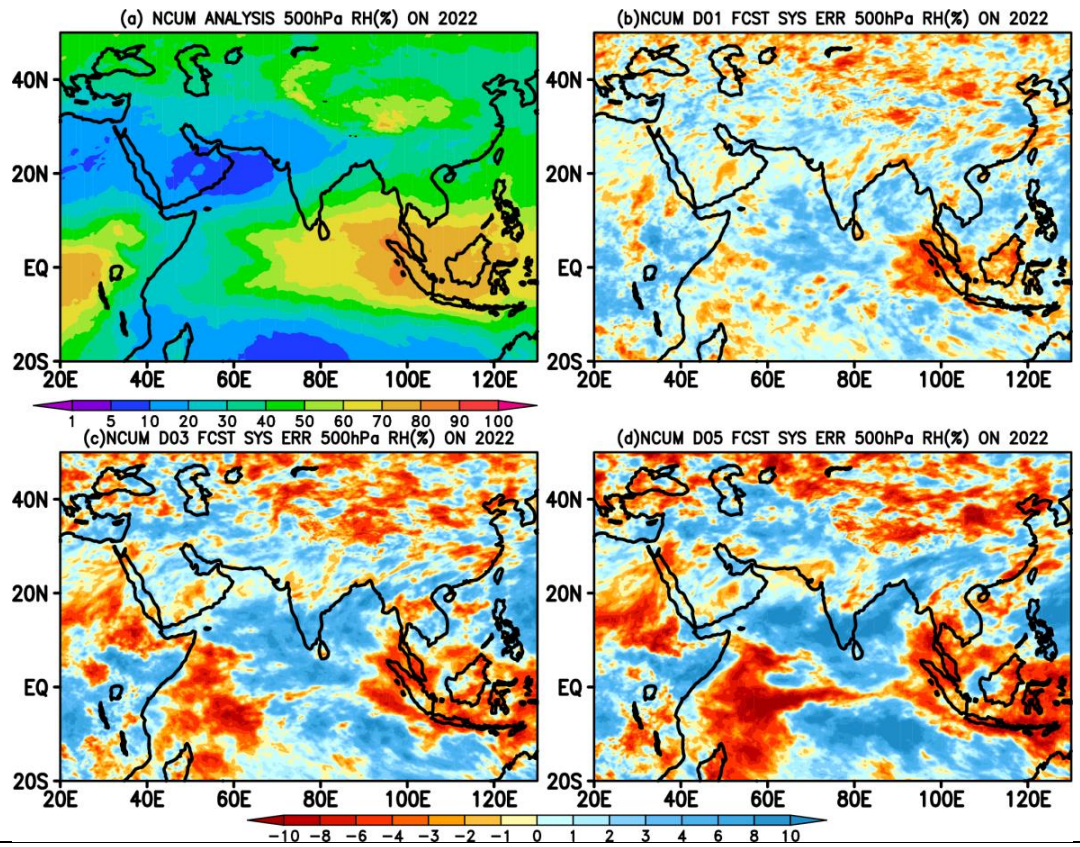


**Figure 17. (a) Mean Relative Humidity (%) and systematic errors (%) in (b) Day-1, (c) Day-3, and (d) Day-5 forecasts at 500 hPa during ON 2022.**

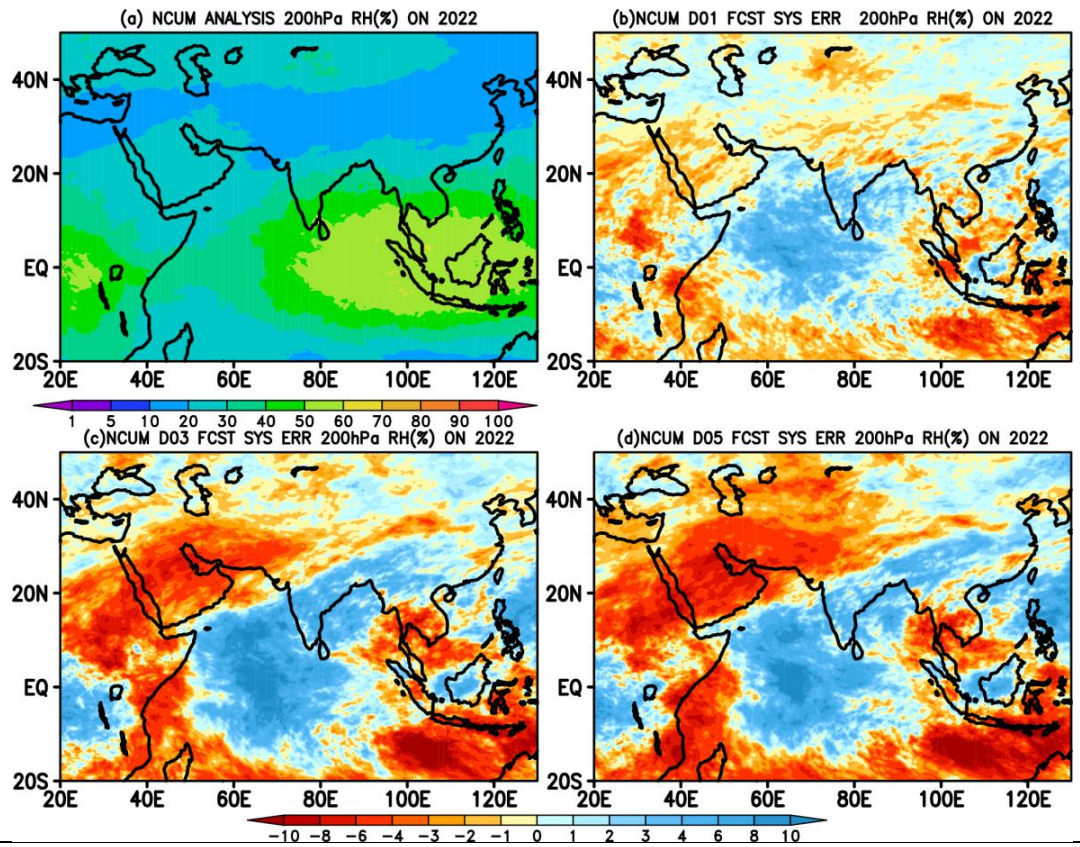


**Figure 18. (a) Mean Relative Humidity (%) and systematic errors (%) in (b) Day-1, (c) Day-3, and (d) Day-5 forecasts at 200 hPa during ON 2022.**

## 4.3. Surface (10m) winds

Seasonal mean winds at 10m from the analysis (Figure 19a) show the presence of strong Northerlies and North easterlies over the Bay of Bengal (BoB) and Arabian Sea (AS), respectively, with maximum winds around open AS, African coast, and South China Sea. Reversal of these north easterlies to westerlies after crossing the equator is also noted in the analysis. The systematic errors in the forecasts (Figures 19 b-d) depict few notable features; 1) Presence of feeble cyclonic circulation over BoB is noticed in Day-1 (Figure 19b). 2) Presence of south-westerlies over AS and BoB in Day-3 and Day-5 (Figures 19c and d). 3) On a similar note, the easterly wind bias seen around the eastern equatorial region is also getting intensified with forecast time.

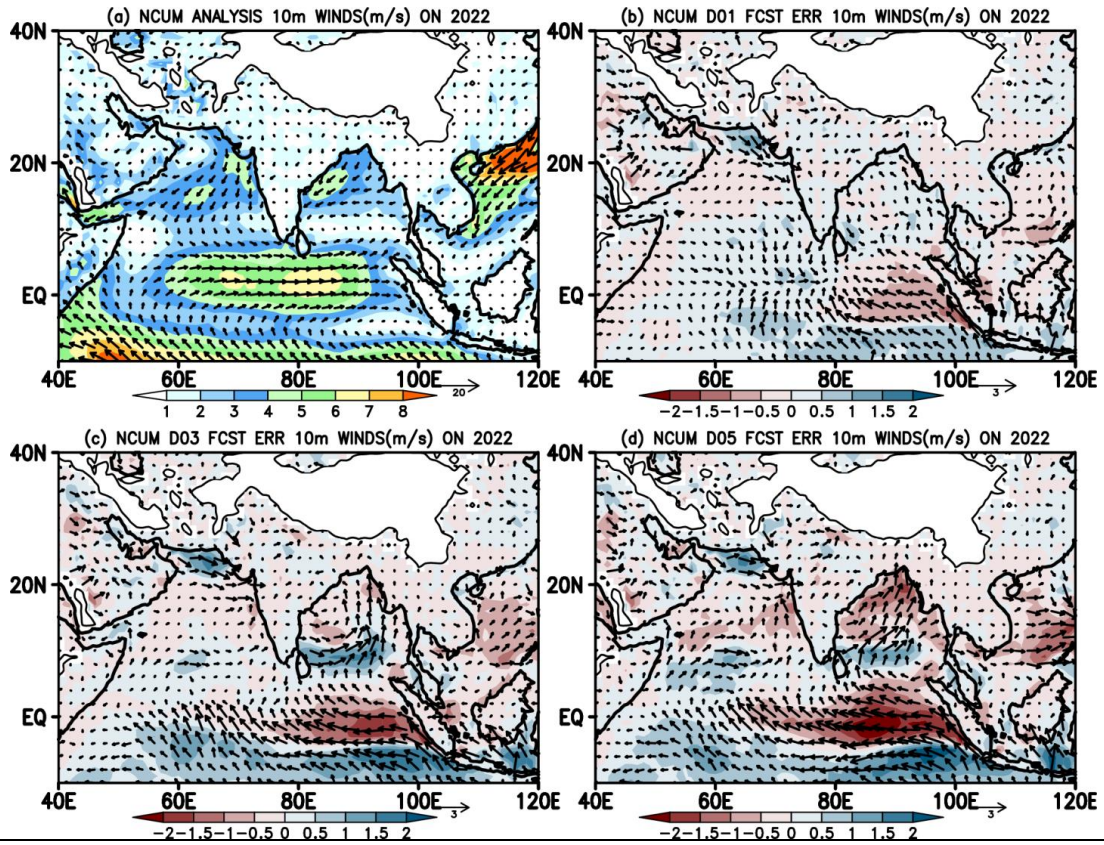


**Figure 19. (a) Mean winds at 10m height and systematic errors (m/s) in (b) Day-1, (c) Day-3, and (d) Day-5 forecasts during ON 2022.**

## 4.4. Temperature at 2m

Seasonal mean temperature ranges between 24-30$^0$C all over the Indian land and surrounding oceanic regions (Figure 20a). Systematic errors (Figures 20b-d) show a relatively cold bias (< -1$^0$C) over Indian land regions and these cold biases are increasing with forecast lead time. This can be attributed to the dry north-westerly winds from the northwest entering into Indian land and north AS (Figure 19). In addition, most of the BoB and MC along with surrounding regions exhibited warm bias in the range of 0-0.5$^0$C in all the forecast lead times. In addition, model temperature errors also exhibit a cold bias over the AS. It is noted that the magnitude of temperature bias is consistent in all the lead times stated here (Figures 20b-d).

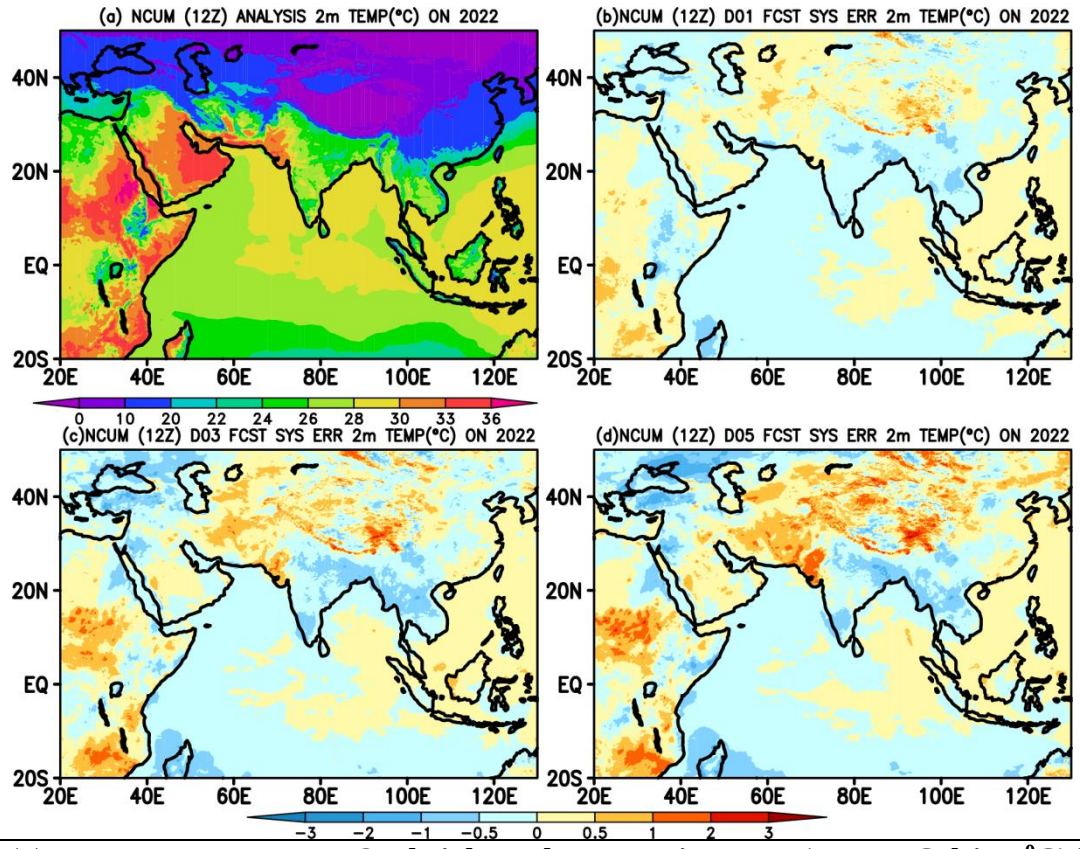


**Figure 20. (a) Mean Temperature at 2m height and systematic errors (Degree Celsius, $^0$C) in (b) Day-1, (c) Day-3, and (d) Day-5 forecasts during ON 2022.**

## 4.5. Total Precipitable Water (PWAT)

Seasonal mean PWAT shows a large value (> 55 mm) around the equatorial regions (Figure 21a), especially over the Maritime continent owing to the presence of winter-time MJO active conditions over these regions. In contrast, most of the northern and central Indian regions are dry with very low PWAT values (5-15 mm). However, extreme southeast peninsular India exhibits moderate PWAT values around 35-40 mm due to the effect of post-monsoon conditions (Figure 21a). Systematic error in PWAT (Figures 21 b-d) shows a column dry over Indian land regions on Day-1, this dryness in column is enhancing with forecast lead time and its magnitude is maximum in Day-5 (Figures 21 c-d). Large positive (negative) PWAT biases are seen over the AS and equatorial (MC) regions. This excess (deficit) column water over the equatorial regions will influence the MJO convection and propagation towards the west Pacific.

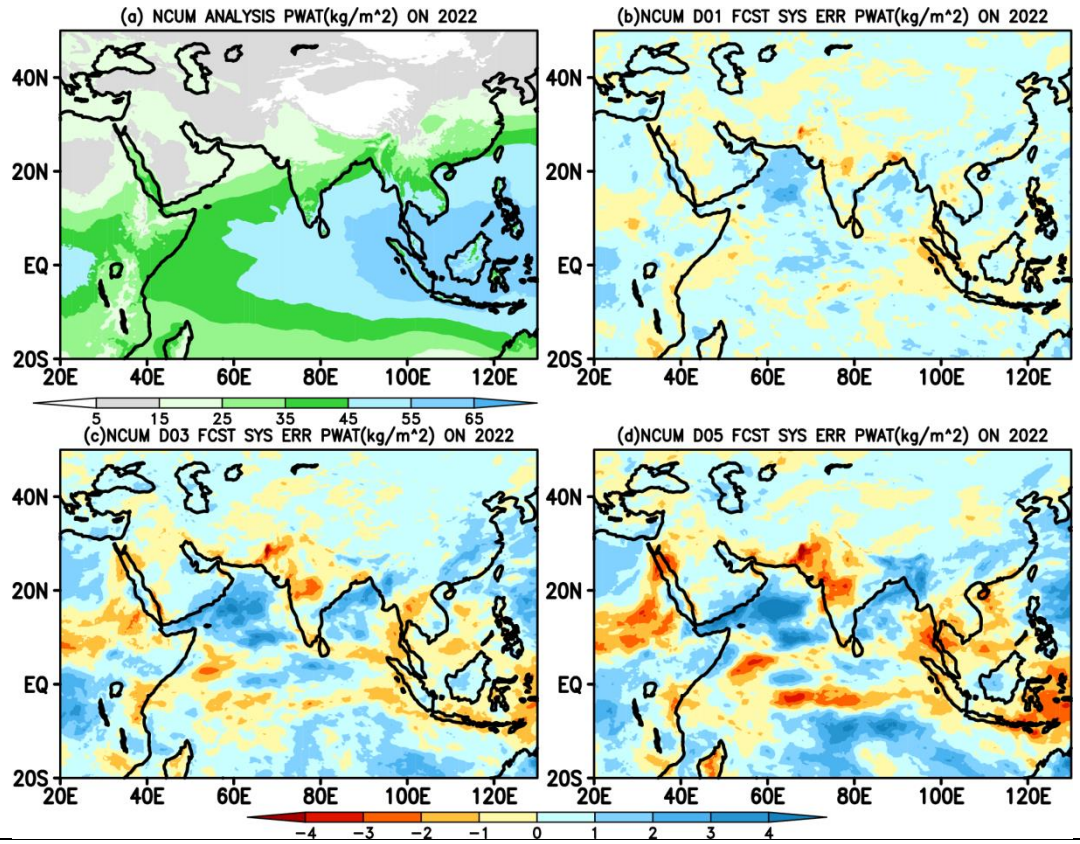


**Figure 21. (a) Mean total precipitable water (PWAT) up to model levels and systematic errors (mm) in (b) Day-1, (c) Day-3, and (d) Day-5 forecasts during ON 2022.**

## 5. Rainfall Forecast Verification during ON 2022

In general, during ON, rainfall primarily occurs over the meteorological sub-divisions of Tamil Nadu, coastal Andhra Pradesh, and parts of Kerala. Nearly 45% of the annual rainfall occurs during this season over these subdivisions. Further, this season is usually considered as cyclone season over the North Indian Ocean (NIO) where the systems move west/northwest-wards affecting the coastal regions of southeast peninsular India. In addition, *Easterly waves* that moves across peninsular India also contribute significantly to the ON rainfall activity. Another important feature is the establishment of a trough in the southern BoB and associated with that we usually see cyclonic circulations. This LP area draws tropical disturbances such as cyclones and easterly waves causing widespread rainfall over Tamil Nadu and neighboring subdivisions. During ON 2022, four low-pressure systems formed over BoB that have influenced the rainfall activity over south peninsular India.

In this section, verification of NCUM-G model rainfall forecasts is presented for ON 2022. The daily accumulated rainfall forecasts are verified against the NCMRWF-IMD merged Satellite and gauge rainfall

product. The discussion presented in this section is confined to mean and mean error (ME) over the India region. Further, this section also quantifies forecast skill using standard verification metrics, namely, the probability of detection (POD), false alarm ratio (FAR), and critical success index (CSI) which are described in standard textbooks (Wilks, 2011, Jolliffe and Stephenson, 2012); and Symmetric extremal dependence index (SEDI), a metric for extreme and rare events (Stephenson et al 2008, Ashrit et al 2015b, Sharma et al 2021).

.

## 5.1. Mean and Mean Error

The observed and forecast mean rainfall during ON 2022 is shown in Figure 22. Observations indicate the highest mean rainfall exceeding 15mm/day is seen over the southern parts of peninsular India, south BoB, and equatorial oceanic regions. Moderate rainfall (2-4 mm/day) is seen over the Jammu and Kashmir regions where the effect of western disturbances is more prominent which brings a significant amount of rain over these regions. The panels in the middle row, Figures 22 b-d show the Day-1, Day-3, and Day-5 NCUM-G forecast rainfall averaged during the ON2022 period. The observed peak in rainfall amounts is well predicted in all the forecast lead times. However, it is found that the NCUM-G forecast overestimates mean rainfall amounts and spatial distribution over the north-eastern regions, BOB, and the oceanic regions around the equator. Apart from this most of the Indian subcontinent is dry with no convection in both observations and forecasts (Figures 22 a-d). Now, to further quantification forecast mean errors (ME) are computed against the observation. The panels in the bottom row show rainfall ME (Figures 22 e-g) in predicted rainfall indicating wet bias (blue) over southern parts of the oceanic regions consistent with the mean rainfall patterns (Figures 22 b-d). Small dry bias regions are noticed over Sri Lanka and some parts of Tamil Nadu in the rainfall forecasts and the magnitude of dry bias is increases with lead time (Figures 22 e-g).

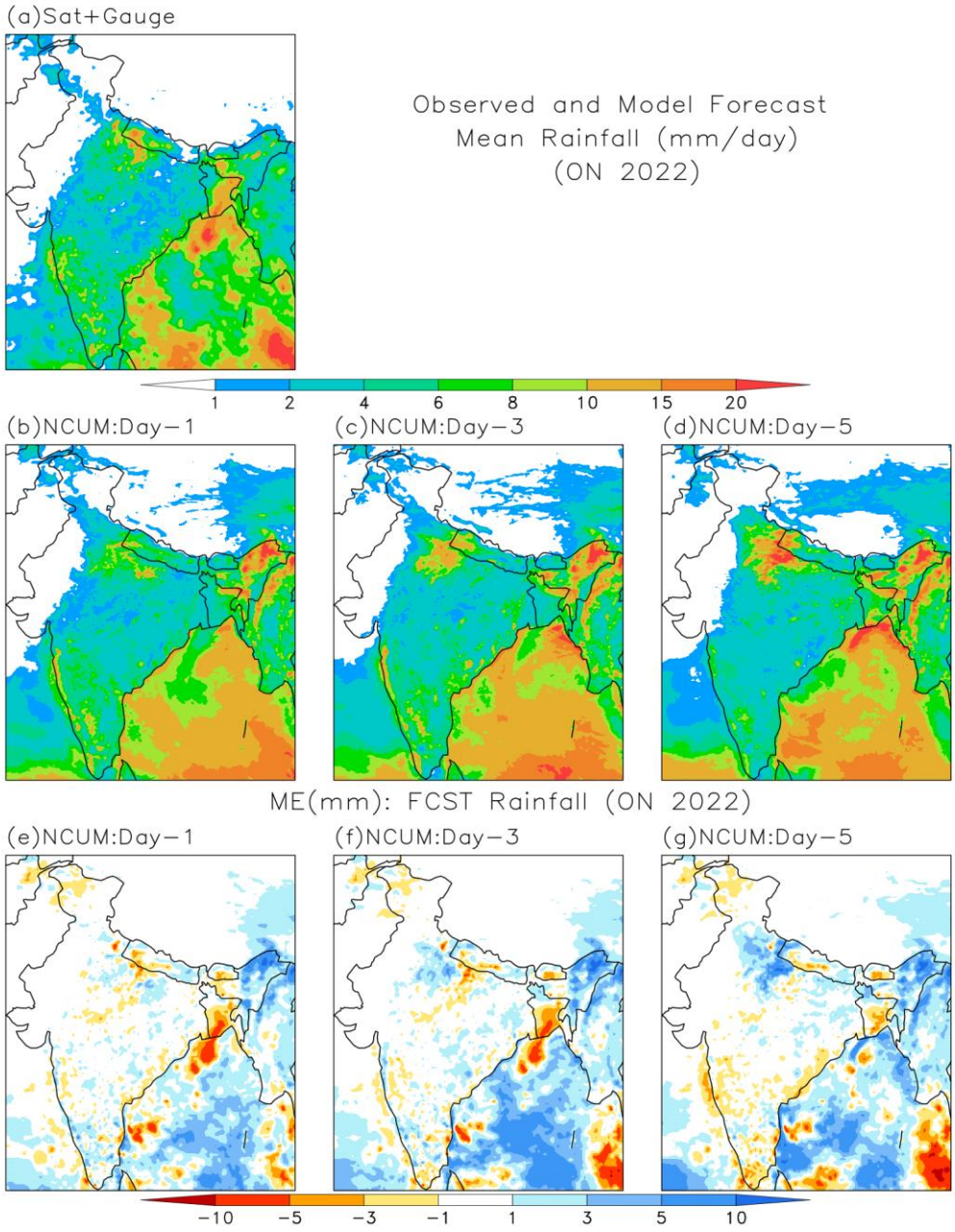


**Figure 22. Accumulated ON rainfall (mm) in (a) Observations and (b) Day-1, (c) Day-3, and (d) Day-5 forecasts. Bottom panels (e), (f), and (g) show Mean Error (ME) in Day-1, Day-3, and Day-5 forecasts, respectively.**

## 5.2. Categorical Scores of Rainfall Forecasts

To further quantifying the model rainfall forecasts, categorical skill scores are computed over the Indian subcontinent (Figure 23). The categorical approach of verifying quantitative precipitation forecast (QPF) is generally based on the 2 x 2 contingency table which is evaluated for each threshold. Verification scores are presented for rainfall of up to 30mm/day. For different rainfall thresholds, POD and FAR show decrease and

increase in scores, respectively. The BIAS score (frequency bias) indicates that forecasts overestimate the frequency up to 9mm/day thresholds. The values of the Peirce's skill score (PSS) and SEDI, all are high for rainfall up to 3-9 mm/day suggesting reasonable skill. PSS score shows a very sharp decrease as the threshold varies. Overall, the skill is not bias-free. For higher rainfall thresholds (> 10 mm/day), frequency bias is almost constant, but the skill is low as indicated by CSI, PSS, and SEDI (Figure 23).

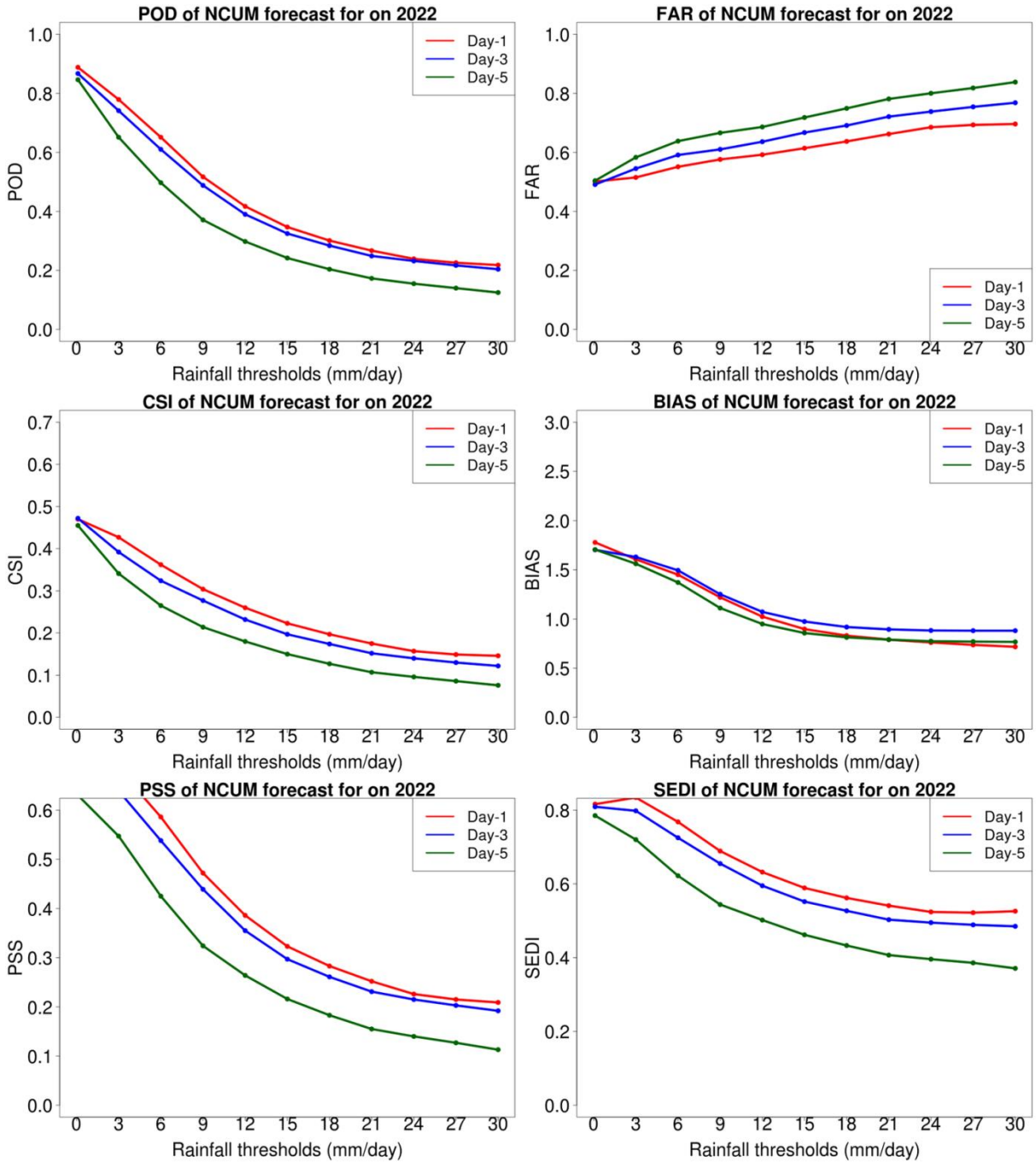


**Figure 23. Categorical all India Rainfall scores POD (*top left*), FAR (*top right*), CSI (*middle left*), BIAS (*middle right*), PSS (*bottom left*), and SEDI (*bottom right*).**

# 6. Significant Weather Events during Oct-Nov 2022

This section provides a brief summary report on the verification of the NCMRWF model forecasts for the recent Cyclonic Storm (CS) 'SITRANG' during 22-25 Oct 2022, which developed over the Bay of Bengal (BoB). Verification of the forecast tracks and intensity is presented for NCMRWF Unified Models; NCUM-G (12km grid resolution), NCMRWF Global Ensemble Prediction System (NEPS-G; 12km grid resolution), NCMRWF Regional Unified Model (NCUM-R; 4km grid resolution) for both 00UTC and 12UTC runs; and NCMRWF Regional Ensemble Prediction System (NEPS-R; 4km grid resolution) for 00UTC runs. Forecast verification is presented for model-predicted tracks and intensity against the IMD best track data.

## 6.1. Bay of Bengal CS 'SITRANG' during 22-25 Oct 2022

### 6.1.1. The bi-variate TC Tracker (MOTC Tracker)

The Met Office bi-variate approach for tracking tropical cyclones (TCs) is used in real-time to track the location and intensity of the system in the models. The bi-variate method identifies TCs by examination of the 850 RV field but then fixes the TC center to the nearest local Mean Sea level Pressure (MSLP) minimum. This is the adopted method at the Met Office, UK. The key advantage of the method is that it gives a strong signal of the approximate center of the TC even for weak systems and does not depend on the '*tc vitals*' information for tracking.

### 6.1.2. Forecast Tracks and Strike Probability

Figure 24 show the observed and predicted tracks based on 12UTC of 20, 21, 22, and 23$^{rd}$ Oct 2022. *The NCUM-G, NEPS-G, and NCUM-R predicted tracks indicate that the system would track towards the Bangladesh coast in each of the forecasts. These were the early indications that the cyclone would approach the coast of Bangladesh. The early tracks based on the 20$^{th}$ and 21$^{st}$ indeed suggest re-curvature over the Sea*. The strike probability (Figure 25) based on the 22-member NEPS-G ensemble indicate that the cyclone would approach the Bangladesh coast in the forecast based on 20$^{th}$ Oct 2022.


**Figure 24. Observed and forecasted tracks of BoB CS 'Satrang' during 20-23May 2022 based on 12UTC**

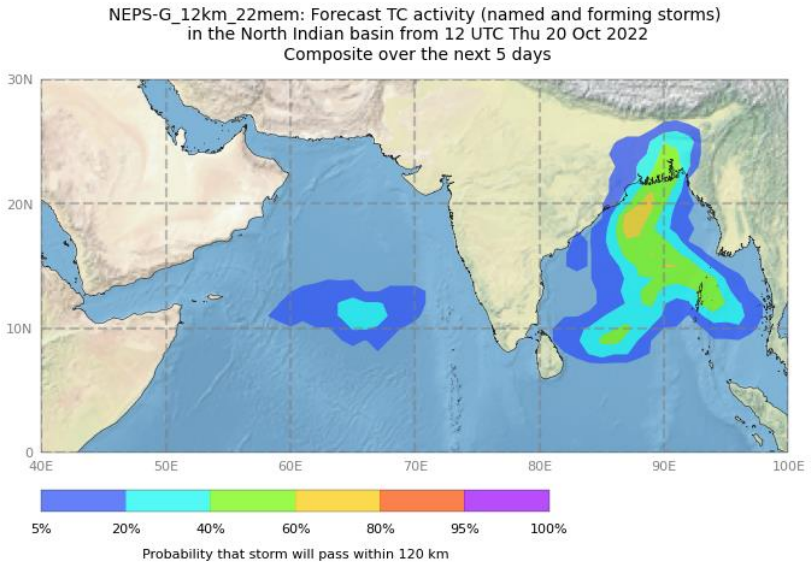


**Figure 25. NEPS-G members strike probability based on 12UTC of 20 Oct 2022.**

### 6.1.3. Forecast Track Errors

Track errors are computed against the IMD's final Best Track data. The forecast tracks based on 00UTC and 12UTC runs (except for NEPS-R) have been used for verification. The NCUM-G (ICs from 17-24 Oct 2022), NEPS-G, NCUM-R (ICs from 21-24Oct 2022), and NEPS-R (ICs 22-24 Oct 2022) have been used in the verification. NCUM-G has the highest number of forecast points verified at higher lead times. Table 1 summarizes the track errors of different models. Mean initial position error is least (88 km) in NEPS-G whereas; the initial error is comparable (104 km) in both NCUM-G and NCUM-R models.

The track error components, Direct Positional Error (DPE), Along Track Error (ATE), and Cross Track Error (CTE) are shown in Figure 26. DPE of NEPS-G up to 48 hrs is relatively lower than other models. DPE in NCUM-G is below 250 km up to 120 hr forecasts. In general, cross track errors are lower than along track errors this resulted due to early prediction of re-curvature in the models.

**Table 1. Forecast Track Errors NCUM-R, NCUM-G, NEPS-R, and NEPS-G (numbers in the adjacent column in italics indicate number of forecast points validated)**

| | DPE | | | | | | | |
|---|---|---|---|---|---|---|---|---|
| **Fcst Hour** | **NCUM-R** | **No of Forecast validated** | **NCUM-G** | **No of Forecast validated** | **NEPS-R** | **No of Forecast validated** | **NEPS-G** | **No of Forecast validated** |
| **0** | 104 | *5* | 104 | *6* | 95 | *2* | 88 | *5* |
| **12** | 101 | *6* | 75 | *6* | 80 | *3* | 60 | *6* |
| **24** | 105 | *5* | 53 | *5* | 62 | *3* | 46 | *6* |
| **36** | 98 | *6* | 96 | *5* | 61 | *2* | 82 | *6* |
| **48** | 124 | *6* | 103 | *6* | 145 | *2* | 97 | *5* |
| **60** | 137 | *5* | 126 | *6* | 53 | *1* | 77 | *4* |
| **72** | 125 | *4* | 155 | *6* | 151 | *1* | 67 | *3* |
| **84** | | | 210 | *6* | | | 191 | *2* |
| **96** | | | 207 | *6* | | | 306 | *1* |
| **108** | | | 184 | *6* | | | | *0* |
| **120** | | | 234 | *5* | | | | *0* |

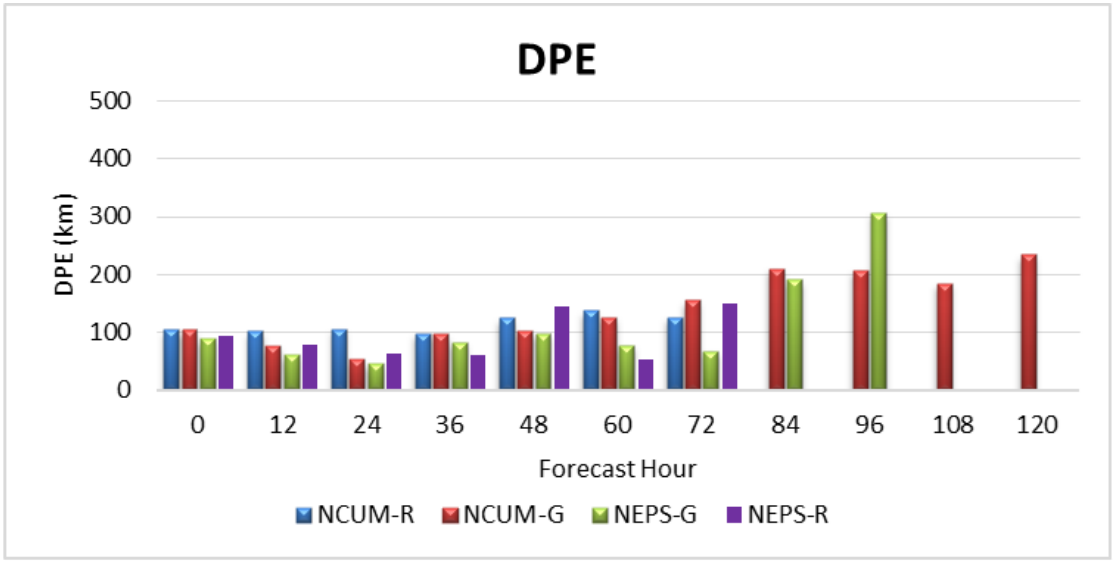


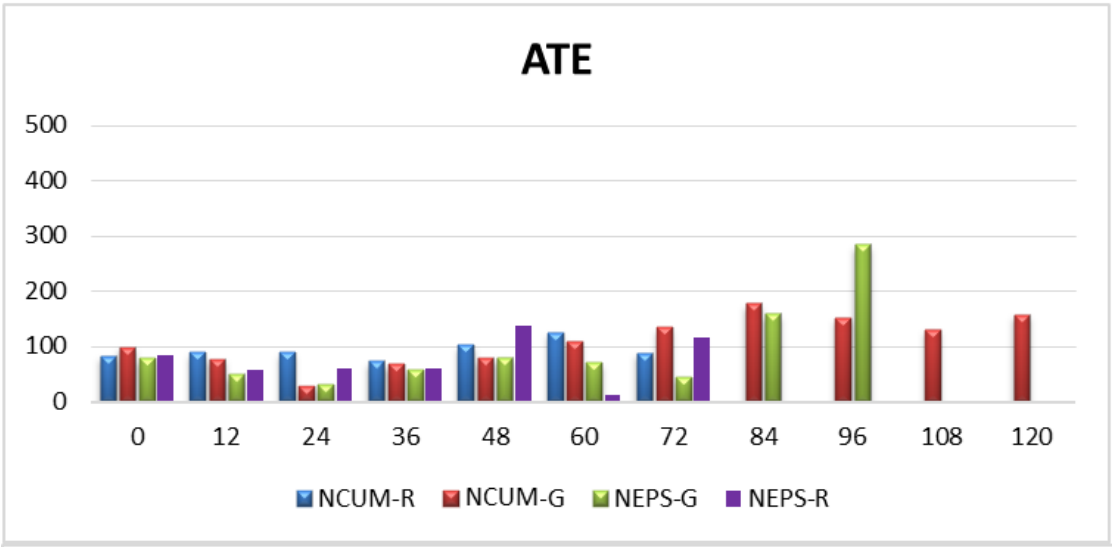


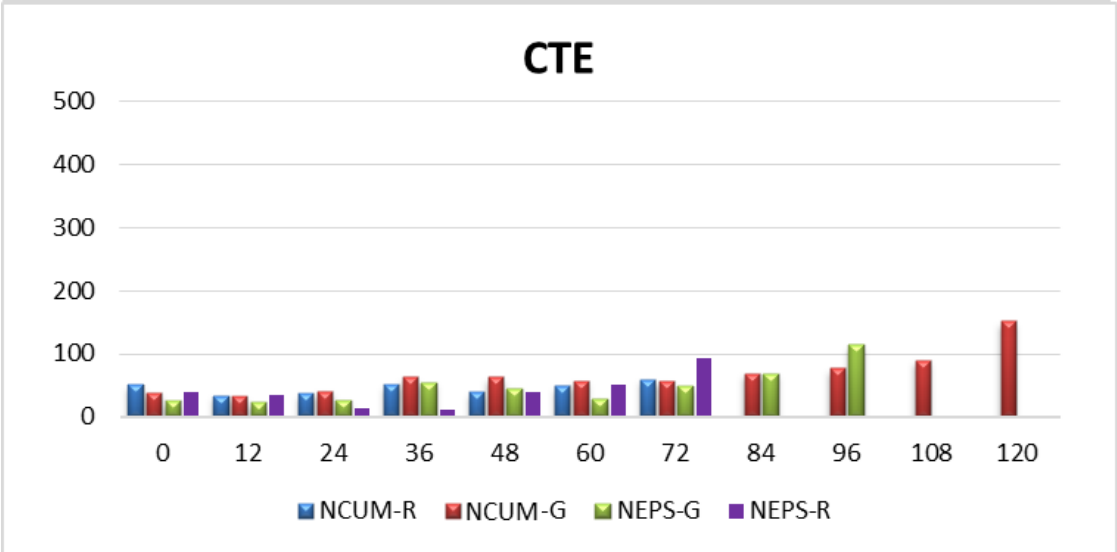


**Figure 26. Track forecast errors (top) Direct Position Error (DPE), (middle) Along Track Error (ATE), and (bottom) Cross Track Error (CTE) in km.**

### 6.1.4. Forecast Intensity Errors (Min SLP and Max Wind)

The mean absolute error (MAE) in the forecast of central pressure (CP) and maximum sustained wind (MSW) for NCUM-R and NCUM-G models is shown in Figure 27. The average error in MSW and CP is lower in NCUM-G up to 72 hr. Forecast MSW from different initial conditions and IMD-BT are shown in Figure 28. NCUM-G intensity has mostly followed the IMD observation having peak intensity on 24th Oct except IC 21st Oct. NCUM-R shows strong positive bias in MSW forecasts (except IC 24th Oct 2022).

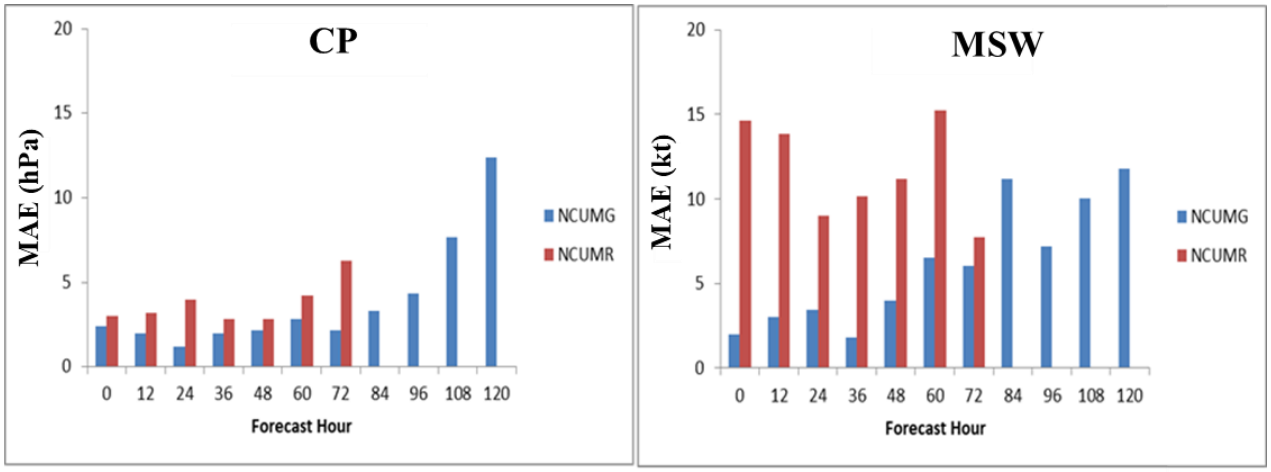


**Figure 27. Mean Absolute Error (MEA) in CP (hPa) and MSW (kt) at different forecast lead times**

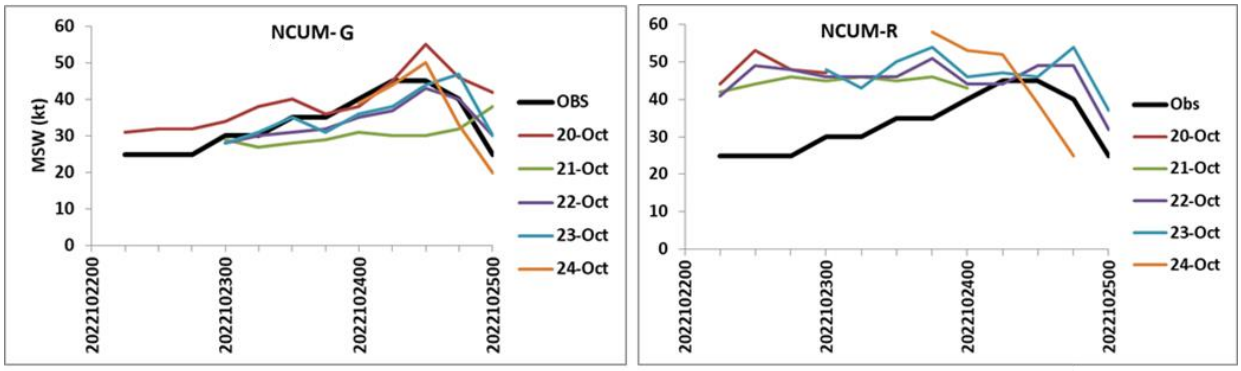


**Figure 28. Intensity given by MSW (kt) in NCUM-G and NCUM-R forecasts with different initial conditions**

### 6.1.5. Verification of Strike Probability

Verification of strike probability is presented using Relative Operating Characteristics (ROC) and Reliability diagram (attributes diagram). The Reliability diagram gives a comparison of forecast probability against the observed frequencies. A perfect match will show all points along the diagonal line. Points above diagonal suggest underestimation (lower forecast probabilities) while points below the diagonal suggest over estimation (higher forecast probabilities).

For the case of CS 'Sitrang', the verification of strike probability obtained from NEPS-G is carried out using the best track data. Figure 29 shows the reliability and ROC plots for the strike probability verification. The model is over forecasting as the observed frequencies are lower than the forecast probabilities. The ROC curves show that the models have skill as the curves are away from the diagonal line of no resolution. Also, the area under the ROC is 0.87 for NEPS-G which shows reasonable skill.

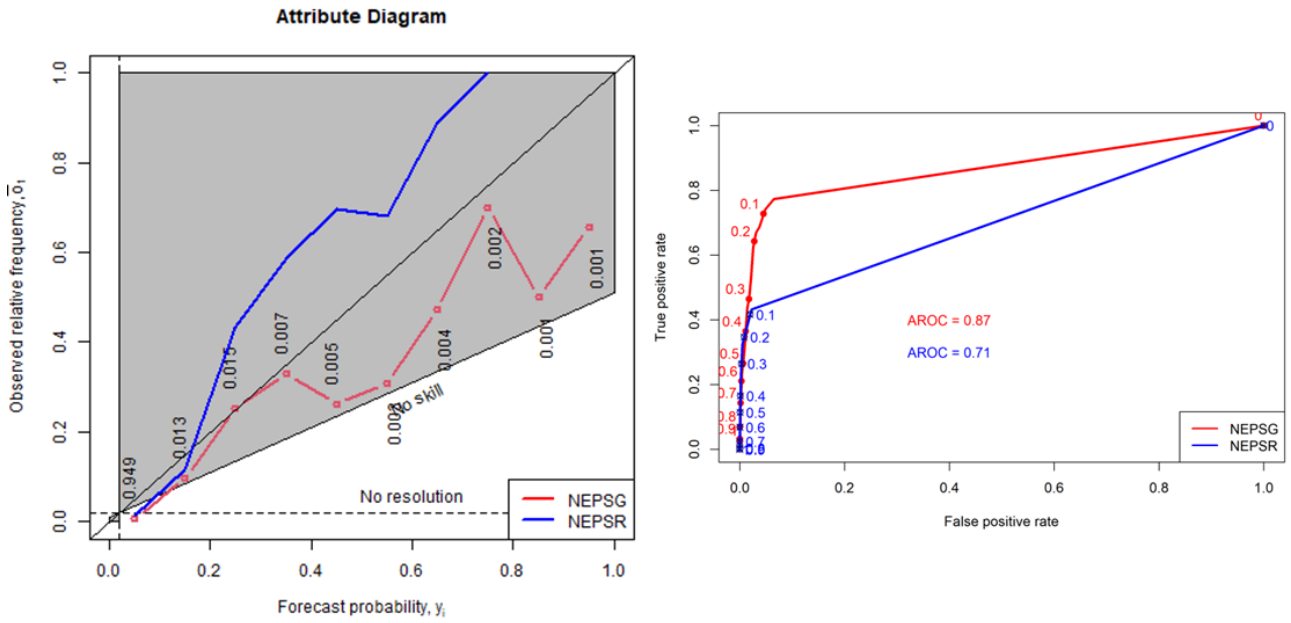


**Figure 29. Verification of strike probability using reliability diagram (left) and ROC curve (right) for the case of CS 'Sitrang'**

## 7. Summary and Conclusions

This report documents performance of the NCMRWF model forecasts during winter season ON 2022. The verification results are presented to address both forecasters and model developers. The information on biases in the forecast winds, temperature, humidity, rainfall, etc., are crucial for the forecasters to interpret the model guidance for forecasting. Additionally, information on recent improvements in the model skill adds to confidence in the model forecasts. The results of the study can be summarized below.

### 7.1. NCUM-G Mean analysis and anomalies during ON 2022

- *The low-level wind anomalies at 850 and 700 hPa levels show the presence of easterly/northeasterly winds indicating the Post-monsoon (ON) over south peninsular India. The ON 2022 anomaly winds show stronger westerlies (easterly anomaly) over the eastern equatorial Indian Ocean (Bay of Bengal). This pattern of anomalies extends up to 500 hPa. At 500 hPa, the deflection of westerlies between 20-40$^0$N and 80-100$^0$E can be seen in the mean winds due to*

*Himalayan topography. The strength for these westerlies is increased from 200 hPa level. The subtropical jet (STJ) is clearly seen at 200 hPa with magnitudes more than 40m/s. The anomalies suggest the weakening of the jet.*

- *Low level (850 hPa) temperature exceeds $18^0$C over the western Indian regions. In contrast to the temperatures at 850 hPa level, temperature distribution is quite homogeneous ranging between 8-$10^0$C, except over the BoB at 700 hPa. This relatively strong heating in the lower troposphere probably enhances the trough and subsequently, the cyclogenesis noted earlier. The temperature anomalies reveal that the above normal temperature over BoB relative to climatological means with magnitudes of $1^0$C is favorable for convective initiation over BoB.*
- *During ON-2022 season lower tropospheric humidity is larger over the southern peninsula India due to the strong easterly flow from BoB to the Indian subcontinent. Also, the high humidity can be noticed over the equatorial Indian Ocean and Maritime Continent (MC). In particular, when we see the anomalous distribution for the ON 2022, the above normal percentage of RH can be clearly visible over BoB and coastal regions around the south peninsular India.*

## 7.2. NCUM-G Systematic Errors

- *Systematic errors in winds at 850 hPa from Day-1 forecasts show an easterly wind bias along equator between 80-$100^0$E. A westerly wind bias over the south Arabian Sea around $60^0$E is seen in Day-1 forecast which is getting enhanced with forecast lead time. An error in low-level winds enhances around the equatorial regions and this could be due to the enhanced convective activity during this season. Similar systematic errors in winds are also noticed at 700 hPa level over the Indian region. Interestingly Day-1 forecast errors are relatively small compared to the Day-3 and Day-5 forecasts. At 500 hPa, errors in winds are relatively small in Day-1 forecasts. The wind bias seen over equatorial regions is enhancing in Day-3 and Day-5 forecasts with westerlies on the west and easterlies on the eastern indicating active convection around equatorial regions. Systematic errors at 200 hPa level winds show enhanced divergent circulation along the equatorial regions on Day-3 and a similar spatial pattern in winds is also seen on Day-5 with enhanced error magnitudes.*
- *Model shows warm bias (~$1^0$C) occupied over northwestern Indian land mass and also over the oceanic regions, and the magnitude of this bias is increasing over land regions with forecast lead time. Interesting to see that the bias at 700 hPa over the equatorial oceanic regions reverse sign and now exhibits cold bias compared to the 850 hPa level. errors in upper-troposphere (200 hPa) temperatures show a large patch of warm bias over the eastern equatorial Indian Ocean (EEIO) and it moving slightly eastward in Day-3 and Day-5 forecasts.*
- *Systematic errors at 850 hPa level show dry bias over the Indian land region, most of the Indian subcontinent, and regions surrounding MC; and this dryness is enhancing with forecasts lead time, which could possibly influence the MJO propagation through MC in NCUM-G. Interestingly the dry bias seen over Indian subcontinent at 850 hPa level changed sign to positive and moist bias is seen at 700 hPa level. However, the dryness over MC and surrounding regions still persists at all the levels from 700 to 200 hPa.*
- *Systematic errors of winds at 10m show the presence of feeble cyclonic circulation over BoB and south-westerlies over AS and BoB in Day-3 and Day-5. On a similar note, the easterly wind bias seen around the eastern equatorial region is also getting intensified with forecast time.*
- *Systematic errors show a relatively cold bias (< -$1^0$C) over Indian land regions and these cold biases are increasing with forecast lead time. This can be attributed to the dry north westerly winds from the northwest entering into Indian land and north AS.*
- *Systematic error in PWAT shows a column dry over Indian land regions in Day-1, this dryness in column is enhancing with forecast lead time and its magnitude is maximum on Day-5. Large positive (negative) PWAT biases are seen over the AS and equatorial (MC) regions. This excess*

*(deficit) column water on the equatorial regions will influence the MJO convection and propagation into the west Pacific.*

## 7.3. Rainfall Forecast Verification

- *NCUM-G forecast overestimates post-monsoon mean rainfall amounts over the north-eastern regions, BOB, and the oceanic regions around the equator. Apart from this, most of the Indian subcontinent is dry with no convection in both observations and forecasts. Small dry bias regions are noticed over Sri Lanka and some parts of Tamil Nadu.*
- *For different rainfall thresholds, POD and FAR show decrease and increase in scores, respectively. The BIAS score (frequency bias) indicates that forecasts overestimate the frequency up to 9mm/day thresholds. The values of PSS and SEDI, all are high for rainfall up to 9 mm/day suggesting reasonable skill. PSS score shows a very sharp decrease as the threshold varies.*

## 7.4. Significant Weather Features during ON 2022

- ***Early Tracks:*** *Forecast tracks based on 12UTC of 20$^{th}$ Oct 2022 predicted that the system would track towards the Bangladesh coast. These early tracks show re-curvature over the Sea.*
- ***Initial Position Error:*** *Mean initial position error is least in NEPS-G (88km).*
- ***Direct Position Error:*** *Up to 48hr forecast mean DPEs are lowest in NEPS-G. NCUM-G errors are below 250 km up to 120 h.*
- ***Intensity verification (NCUM-G & NCUM-R):*** *The MAE in both CP and MSW is higher in NCUM-R (overestimation of intensity) up to 72 hrs.*
- ***Verification of strike probability (NEPS-G & NEPS-R):*** *ROC and Reliability diagrams are used for this purpose. The reliability curve for NEPS-G shows over forecasting as the curve is below the diagonal line whereas, for NEPS-R the model shows under forecasting of the strike probabilities. However, for forecasts made with lower probabilities (<0.5) the NEPS-G curve is seen to be closer to the diagonal as compared to NEPS-R. On comparing the ROC curves, it is seen that the for NEPS-G the curve is closer to the top left diagonal indicating better resolution in the NEPS-G as compared to NEPS-R. Also, this shows that the Hit Rate for NEPS-G is higher than NEPS-R. Also, the AROC is higher for NEPS-G (0.87) as compared to NEPS-R (0.71)*

## References


1. Ashrit R, Sharma K, Dube A, Iyengar G R, Mitra A K and Rajagopal E N 2015b: Verification of short-range forecasts of extreme rainfall during monsoon; Mausam 66 375–386, 607.
2. Barker, D., 2011. Data assimilation-progress and plans, MOSAC-16, 9-11 November 2011, Paper16.6.
3. Hersbach H, Bell B, Berrisford P, et al. 2020: The ERA5 global reanalysis. Q J R Meteorol Soc. 2020;146:1999–2049. https://doi.org/10.1002/qj.3803
4. Jolliffe, I. T., and D. Stephenson, 2012: Forecast Verification: A Practitioner's Guide in Atmospheric Science, John Wiley & Sons, Ltd.
5. Kumar Sumit, A. Jayakumar, M. T. Bushair, Buddhi Prakash J., Gibies George, Abhishek Lodh, S. Indira Rani, Saji Mohandas, John P. George and E. N. Rajagopal 2018: Implementation of New High Resolution NCUM Analysis-Forecast System in Mihir HPCS. NMRF/TR/01/2019, 17p.
6. Kumar Sumit, M. T. Bushair, Buddhi Prakash J., Abhishek Lodh, Priti Sharma, Gibies George, S. Indira Rani, John P. George, A. Jayakumar, Saji Mohandas, Sushant Kumar, Kuldeep Sharma, S. Karunasagar, and E. N. Rajagopal 2020: NCUM Global NWP System: Version 6 (NCUM-G:V6), NMRF/TR/06/2020.
7. Kumar Sumit, Gibies George, Buddhi Prakash J., M. T. Bushair, S. Indira Rani and John P. George 2021: NCUM Global DA System: Highlights of the 2021 upgrade, NMRF/TR/05/2021.
8. M. Rajeevan, C.K. Unnikrishnan, J. Bhate, K. Niranjan Kumar, P.P. Sreekala Northeast monsoon over India: variability and prediction Met. Apps, 19 (2012), pp. 226-236
9. Mitra, A. K., A. K. Bohra, M. N. Rajeevan and T. N. Krishnamurti, 2009: Daily Indian precipitation analyses formed from a merged of rain-gauge with TRMM TMPA satellite derived rainfall estimates, J. of Met. Soc. of Japan, 87A, 265-279.
10. Mitra, A. K., I. M. Momin, E. N. Rajagopal, S. Basu, M. N. Rajeevan and T. N. Krishnamurti, 2013, Gridded Daily Indian Monsoon Rainfall for 14 Seasons: Merged TRMM and IMD Gauge Analyzed Values, J. of Earth System Science, 122(5), 1173-1182.
11. Sharma, K., Ashrit, R., Kumar, S. et al. Unified model rainfall forecasts over India during 2007–2018: Evaluating extreme rains over hilly regions. J Earth Syst Sci 130, 82 (2021). https://doi.org/10.1007/s12040-021-01595-1
12. Srivastava A K, Rajeevan M and Kshirsagar S R 2009: Development of a high resolution daily gridded temperature data set (1969–2005) for the Indian region; Atmos. Sci. Lett. 10 249–254, https://doi.org/10.1002/asl.232
13. Stephenson D.B., B. Casati, C.A.T. Ferro and C.A. Wilson, 2008: The extreme dependency score: a non-vanishing measure for forecasts of rare events. Meteorol. Appl., 15, 41-50.
14. Walters, D., and co-authors: The Met Office Unified Model Global Atmosphere 6.0/6.1 and JULES Global Land 6.0/6.1 configurations, Geosci. Model Dev., 10, 1487–1520, https://doi.org/10.5194/gmd-10-1487-2017, 2017.
15. Wilks D S 2011 (eds) Statistical methods in the atmospheric 807 sciences; 3rd edn, Elsevier, 676p